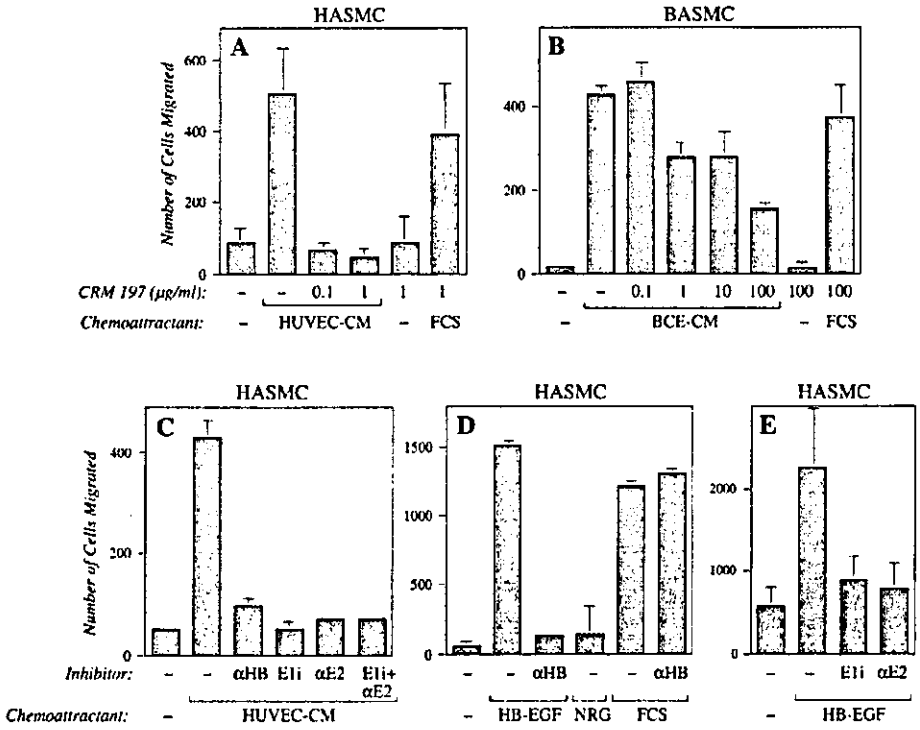

Figure 5. Role of HB-EGF signaling in EC-stimulated SMC migration. The effect of specific inhibitors of HB-EGF signaling on stimulated SMC migration was analyzed using Boyden chamber assays. The inhibitors tested were an HB-EGF inhibitor CRM 197, a neutralizing anti-HB-EGF antibody (αHB), a tyrosine kinase inhibitor of ErbB1 PD 153035 (Eli), and an inhibitory antibody for ErbB2 Herceptin (αE2). The inhibitors were assayed for HASMC migration stimulated by HUVEC conditioned medium (*A*, *C*), on BASMC migration stimulated by BCE conditioned medium (*B*), on HASMC migration stimulated by 20 ng/mL HB-EGF (*D*, *E*), or on HASMC (*A*, *D*) or BASMC (*B*) migration stimulated by 1% FCS. 20 ng/mL NRG-1 was analyzed for its effect as a chemoattractant for HASMCs (*D*). CM, conditioned medium.

lated migration of SMCs, conditioned media from ECs were supplemented with increasing concentrations of CRM 197, a specific inhibitor of HB-EGF (27, 28). The media were then analyzed for their ability to stimulate SMC migration using Boyden chamber assays. CRM 197 inhibited the EC-stimulated migration of both HASMCs and BASMCs in a dose-responsive manner (**Fig. 5*A*, *B***). However, significant quantitative differences were observed when different EC and SMC types were tested: A CRM 197 concentration of 0.1 μg/mL was enough to totally block the migration of HASMCs stimulated by HUVEC conditioned medium (Fig. 5*A*). In contrast, the highest CRM 197 concentration tested, 100 μg/mL, was able to block 65% of BASMC migration stimulated by BCE conditioned medium (Fig. 5*B*). CRM 197 did not block basal SMC migration or migration stimulated by 1% FCS (Fig. 5*A*, *B*), demonstrating specificity of the effect.

The results obtained with CRM 197 were further confirmed using an antibody that neutralizes the bioactivity of human HB-EGF (R&D). The neutralizing antibody blocked 90% of HASMC migration stimulated by the medium (Fig. 5*C*). Consistent with the expression (Fig. 3) and activation (Fig. 4*B*) of HB-EGF receptors ErbB1 and ErbB2 in HASMCs, a small molecular weight tyrosine kinase inhibitor of ErbB1 (PD 153035) and an inhibitory antibody recognizing human ErbB2 (Herceptin) also blocked the HUVEC medium-stimulated migration (Fig. 5*C*). The inhibition was total when the ErbB1 and ErbB2 inhibitors were administered alone or in combination (Fig. 5*C*). These results indicate that HB-EGF is necessary for efficient EC-stimulated migration of vascular SMCs in vitro and that the response requires both ErbB1 and ErbB2.

HB-EGF is sufficient for stimulating SMC migration in vitro

To address whether HB-EGF alone is sufficient to stimulate the migration of SMCs in vitro, recombinant human HB-EGF was tested as a chemoattractant in the Boyden chamber assay. Recombinant HB-EGF stimulated the migration of HASMCs and BASMCs in a dose-dependent manner, with the maximal effect at 20 ng/mL (Fig. 5*D* and data not shown). As expected from ErbB expression and activation analyses (Figs. 3 and 4), 20 ng/mL recombinant NRG-1 did not affect HASMC migration (Fig. 5*D*). The neutralizing anti-HB-EGF antibody (Fig. 5*D*), the ErbB1 inhibitor PD 153035 (Fig. 5*E*), and the neutralizing anti-ErbB2 antibody (Fig. 5*E*) efficiently blocked HASMC migration stimulated by recombinant HB-EGF, indicating that HB-EGF signaling via ErbB1 and ErbB2 was mediating the effect. The neutralizing anti-HB-EGF antibody did not have an effect on the migration stimulated by 1% FCS (Fig. 5*D*), suggesting that the recombinant HB-EGF preparation was free of contaminating stimulatory factors and that the effect of the antibody was specific (Fig. 5*D*).

Angiopoietin-1 stimulates expression of HB-EGF in ECs

Angiopoietins have been shown to regulate the recruitment of PCs or SMCs toward ECs during angiogenesis (4). Since all known angiopoietins function through the EC-specific Tie2 receptor, it has been proposed that they exert their SMC recruiting activity indirectly by stimulating the production of SMC chemoattractants from ECs (2).

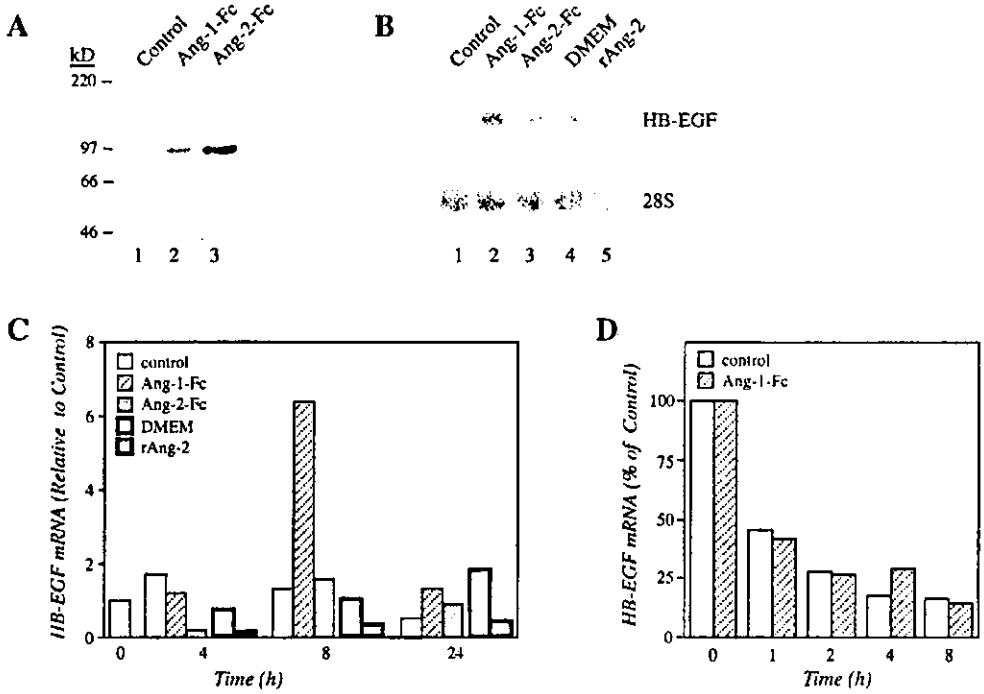

Figure 6. Regulation of HB-EGF mRNA expression in HUVECs by angiopoietins. *A)* Secretion of Ang-1-Fc (lane 2) and Ang-2-Fc (lane 3) proteins to 20-fold concentrated conditioned media from transfected HEK293 cells, but not to concentrated medium from wild-type HEK293 cells (control; lane 1), was demonstrated by Western analysis using an anti-Fc antibody. *B)* Confluent HUVEC cultures were exposed to the concentrated control (lane 1), Ang-1-Fc (lane 2), or Ang-2-Fc (lane 3) media, DMEM (lane 4), or recombinant Ang-2 (lane 5) for 8 h. Total cellular RNA was isolated and analyzed by Northern blot using cDNA probes specific for human HB-EGF (top) or 28S rRNA (bottom). *C)* Northern analysis similar to that described in panel *B* was carried out after stimulating HUVECs for 0, 4, 8, or 24 h. Hybridization signals were quantitated and values obtained for HB-EGF were normalized with the values obtained for 28S rRNA. The experiment was repeated three times with similar results. *D)* Half-life of HB-EGF mRNA was analyzed by real-time RT-PCR at time points after stimulating HUVEC cultures for 8 h with concentrated Ang-1-Fc or control media, followed by inhibition of RNA synthesis with actinomycin D.

To analyze the effects of angiopoietins on endothelial HB-EGF mRNA expression, fusion proteins of Ang-1 or Ang-2 coupled to the Fc fragment of human immunoglobulin gamma (Ang-1-Fc or Ang-2-Fc, respectively) were produced in HEK293 cells. The presence of Ang-Fc proteins in 20-fold concentrated conditioned media from Ang-Fc-producing cells, but not in control medium from wild-type HEK293 cells, was confirmed by Western blot (**Fig. 6*A***). Serum-starved HUVEC cultures were then exposed to Ang-Fc or control medium or to 750 ng/mL of recombinant Ang-2 (from R&D), for 8 h and analyzed by Northern blot using an HB-EGF-specific probe. Ang-1-Fc up-regulated the expression of a single 2.5 kb HB-EGF transcript (Fig. 6*B*, lane 2). In contrast, neither Ang-2-Fc (Fig. 6*B*, lane 3) nor recombinant Ang-2 (Fig. 6*B*, lane 5) had a stimulatory effect on HB-EGF mRNA levels when compared with control medium from HEK293 cells (Fig. 6*B*, lane 1) or DMEM (Fig. 6*B*, lane 4), respectively. Quantitation and time course analysis of the HB-EGF Northern data indicated that *1)* Ang-1-Fc stimulated HB-EGF mRNA expression maximally by 6.4-fold, *2)* the maximal effect was reached at 8 h, and *3)* Ang-2-Fc and recombinant Ang-2 down-regulated rather than stimulated HB-EGF mRNA expression in HUVECs within the time range analyzed (Fig. 6*C*). Similar data were observed when HB-EGF mRNA was quantitated using real-time RT-PCR (data not shown). Furthermore, real-time RT-PCR analysis of the stability of the HB-EGF mRNA in HUVECs demonstrated similar half-lives (≈1 h) for HB-EGF mRNA after an 8 h stimulation with either Ang-1-Fc or control HEK293 medium (Fig. 6*D*), suggesting that Ang-1 regulates HB-EGF expression at a transcriptional level. Consistent with its function as an Ang-1 antagonist for blood ECs, purified recombinant Ang-2 (R&D) was able to block the effect of Ang-1-Fc medium on HB-EGF expression in a dose-responsive manner (50% inhibition at 100 ng/mL, 80% inhibition at 1000 ng/mL), indicating that the activity of Ang-1-Fc medium was specific.

To analyze the effect of Ang-1 on endothelial HB-EGF protein expression, 70% confluent HUVEC cultures were infected with adenoviruses encoding human Ang-1 (AdAng-1) or β-galactosidase (AdLacZ). Three days after infection, the expression of HB-EGF protein was detected by Western blot. AdAng-1 up-regulated HB-EGF protein expression (**Fig. 7*A***, lanes 1 and 2) by 5.6-fold as demonstrated by densitometric analysis of the Western film (Fig. 7*A*, columns). These data demonstrate that Ang-1 is capable of up-regulating the expression of HB-EGF in ECs.

Angiopoietin-1 enhances EC-stimulated migration of SMCs in a mechanism involving HB-EGF

To more directly assess the role of HB-EGF in mediating the effect of Ang-1 on SMC migration, serum-free conditioned media from HUVECs infected with either

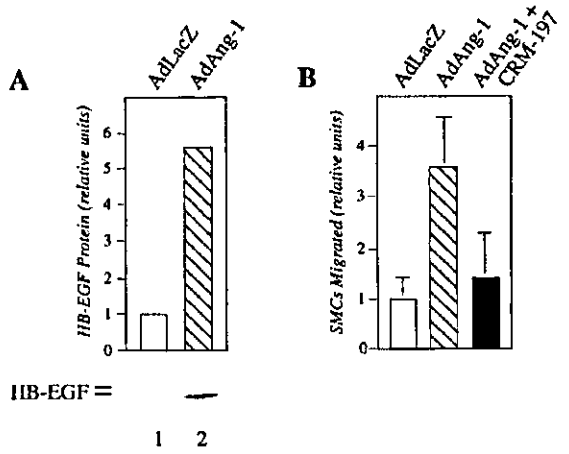

Figure 7. Regulation of HB-EGF protein expression and SMC migration-inducing activity in HUVECs by adenoviral angiopoietin-1. *A)* The expression of HB-EGF protein 72 h after infection of HUVECs with AdLacZ (lane 1) or AdAng-1 (lane 2) was analyzed by Western blot using an anti-HB-EGF antibody (C-18; Santa Cruz). Densitometric quantitation of the HB-EGF-specific bands is shown. *B)* Serum-free conditioned media were collected 48 h after infection of HUVECs with AdLacZ (white bar) or AdAng-1 (hatched bar) and analyzed in Boyden chamber assays for their potential to stimulate HASMC migration. To assess the role of HB-EGF, 1 μg/mL of CRM 197 was added to the medium from AdAng-1-infected cells (black bar).

AdAng-1 or AdLacZ were tested for chemoattractive potential for HASMCs in Boyden chamber assays. AdAng-1 infection up-regulated the capacity of HUVECs to attract HASMCs by 3.2- to 5.6-fold in three independent experiments (Fig. 7*B*). Similar observations were made when HUVEC conditioned media were analyzed after a 24 h treatment with 200 ng/mL recombinant Ang-1 (R&D; data not shown). When 1 μg/mL of the HB-EGF inhibitor CRM 197 was added to the conditioned medium from AdAng-1-infected HUVECs, the capacity of the medium to stimulate SMC migration was reduced by ≈60% (Fig. 7*B*). These findings demonstrate that Ang-1 enhances SMC migration stimulated by ECs in vitro and suggest that a major proportion of this enhancement is mediated via EC-derived HB-EGF.

HB-EGF is expressed in ECs associated with vascular SMCs or PCs in vivo

To study whether HB-EGF is expressed by ECs in angiogenic tissues in vivo, paraffin sections of a 10-wk-old aborted human fetus were immunostained with a chicken polyclonal antibody against the cytoplasmic domain of the mature transmembrane form of human HB-EGF. A positive signal was observed in ECs in a majority of developing vascular structures, including arterial and venous vessels as well as capillaries, in several tissues (**Fig. 8*A*, *E***). As expected based on several previous reports, muscle tissues, including vascular smooth muscle, were slightly positive for HB-EGF. Identical staining patterns were seen when *1)* adjacent sections were stained using an independent anti-HB-EGF antibody recognizing human HB-EGF (C-18) and *2)* sections of mouse embryos (embryonic day 14.5) were stained with an antibody recognizing mouse HB-EGF (M-18) (data not shown). No specific staining was observed when chicken preimmune serum IgG fraction was used (Fig. 8*B, F, J*) or when primary antibody was omitted from the protocol (data not shown).

To confirm the identity of HB-EGF-positive cells, ECs and SMCs/PCs were visualized from adjacent sections by staining with antibodies raised against CD34 (Fig. 8*C, G, K*) and α-SMA (Fig. 8*D, H, L*), respectively. Strong HB-EGF immunoreactivity seemed to colocalize with ECs of vascular structures containing α-SMA-positive SMCs or PCs. For example, ECs in capillaries and venules in the developing skin were HB-EGF positive (Fig. 8*E*) and associated with scattered SMCs/PCs (Fig. 8*H*). In contrast, similar-sized hyaloid vessels in the developing eye were significantly less stained, if stained at all, with anti-HB-EGF antibody (Fig. 8*I*) and were not associated with any detectable α-SMA reactivity (Fig. 8*L*). This is consistent with the later regression of the hyaloid vessels from the developing vitreous (38) and with the role of EC-derived HB-EGF in SMC/PC recruitment during angiogenesis in vivo.

DISCUSSION

We have investigated the role of ErbB receptors and their EGF-like growth factor ligands in the paracrine signaling between ECs and SMCs. Evidence is provided demonstrating that HB-EGF is a central mediator of this interaction. HB-EGF was *1)* expressed by primary HUVECs and *2)* stimulated tyrosine phosphorylation and migration in both HASMCs and BASMCs. Moreover, *3)* HASMCs and BASMCs expressed receptors ErbB1 and ErbB2, which are known to form a high-affinity receptor for HB-EGF (39), *4)* recombinant HB-EGF stimulated tyrosine phosphorylation of ErbB1 and ErbB2 in HASMC, and *5)* reagents that specifically neutralize the activity of either HB-EGF, ErbB1, or ErbB2 blocked the SMC migration-inducing activity secreted by ECs. In addition, *6)* Ang-1, an EC-specific growth factor necessary for efficient SMC recruitment in vivo (8), up-regulated the expression of HB-EGF mRNA and protein in ECs and *7)* enhanced the SMC migration-inducing activity of ECs by a mechanism largely dependent on HB-EGF. Finally, *8)* HB-EGF was expressed in ECs associated with vascular SMCs/PCs during angiogenesis in vivo. These data support a role for HB-EGF, and its receptors ErbB1 and ErbB2, in the recruitment of SMCs by ECs.

SMC recruitment to newly formed vessels has been proposed to involve soluble EC-derived chemoattractants that interact with specific receptors on SMC surfaces (2). We have analyzed the communication between ECs and SMCs by measuring the potential of either cell type to stimulate the migration of the other

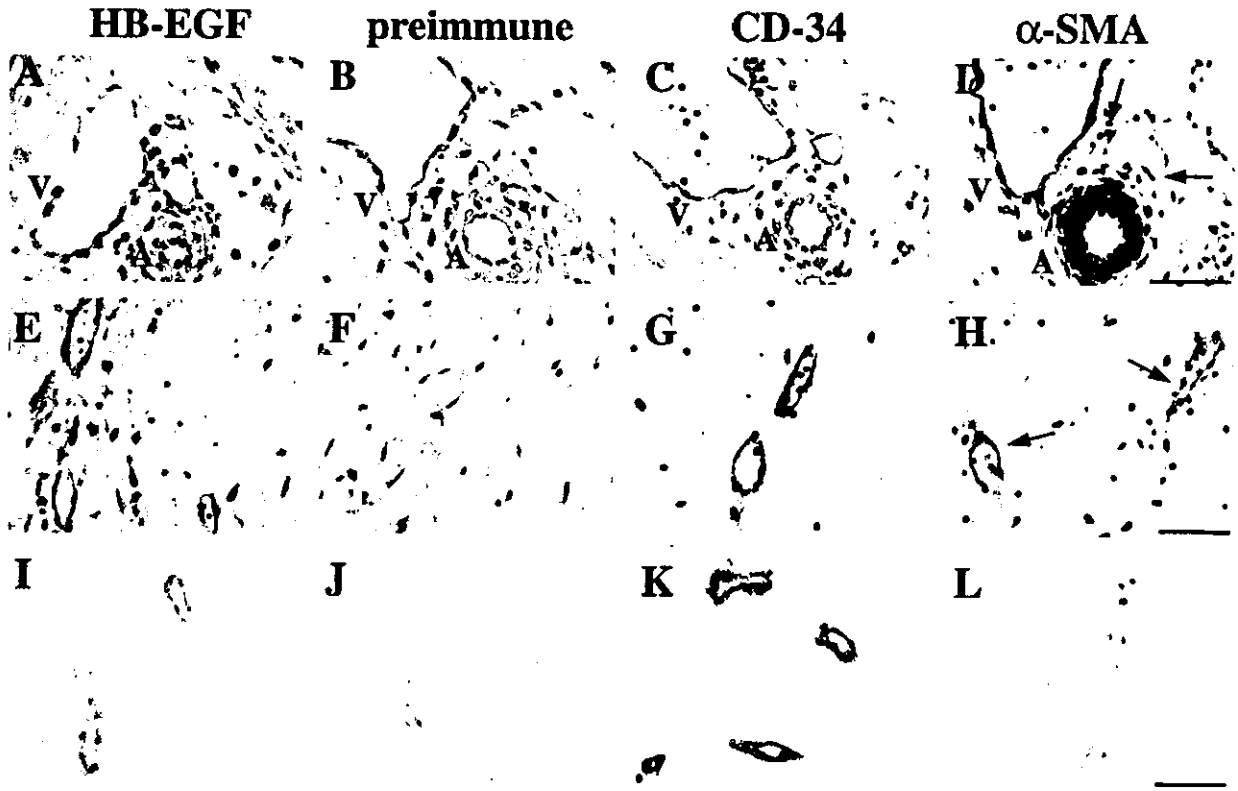

Figure 8. Immunohistochemical localization of HB-EGF in vascular structures during angiogenesis. Paraffin sections of a 10-wk-old human fetus were immunostained with a polyclonal anti-HB-EGF antibody (*A, E, I*), preimmune IgG fraction (*B, F, J*), anti-CD34 (*C, G, K*), or anti-α-SMA (*D, H, L*). Intercostal tissue (*A–D*), dermis of the skin (*E–H*), and vitreous of the eye (*I–L*) are shown from adjacent sections. Arrows point to vessels covered by α-SMA-positive cells (*D, H*) and stain positively with anti-CD34 (*C, G*) and anti-HB-EGF (*A, E*), but not with preimmune IgG (*B, F*). Similar sized hyaloid vessels in the eye, although CD34 positive (*K*), are not stained with anti-α-SMA (*L*) or preimmune IgG (*J*) and demonstrate little if any HB-EGF positivity (*I*). A, developing artery; V, developing vein. Bar, 50 μm.

in vitro. It was demonstrated using Boyden chamber migration assays that conditioned media from primary ECs stimulated the migration of vascular SMCs but that conditioned media from SMCs did not stimulate the migration of ECs. These findings indicate that our in vitro experiments provided a relevant model to characterize the paracrine factors that ECs use to recruit SMCs.

It was demonstrated by RT-PCR that at least two EGF-like ligands are expressed by primary HUVECs: NRG-1 and HB-EGF. Of the two factors detected in HUVECs, NRG-1 is unlikely to mediate signaling from ECs to SMCs since *1)* neither HASMCs nor BASMCs expressed the NRG-1 receptors ErbB3 or ErbB4. SMCs did not respond to recombinant NRG-1 by *2)* protein tyrosine phosphorylation, *3)* specific phosphorylation of ErbB1 or ErbB2, or *4)* migration. Together with observations of the in vivo angiogenic effect of NRG-1 (40) (E. Iivanainen et al., unpublished results), these results imply a role for NRG-1 in vascular biology that is distinct from stimulating recruitment of SMCs. Several lines of evidence, however, support a role of EC-derived HB-EGF in EC–SMC interaction. Both HB-EGF mRNA and protein have been shown to be expressed by HUVECs in vitro (41, 42). Here we demonstrated that HB-EGF is expressed in ECs associated with SMCs/PCs during embryogenesis in vivo. HASMCs and BASMCs were also shown to express HB-EGF receptors and to respond to recombinant HB-EGF by protein tyrosine phosphorylation, migration, and proliferation (data not shown). These findings are in accordance with HB-EGF's well-established role as a potent mitogen and chemoattractant for different types of SMCs (43), including vascular SMCs (33, 44).

The immunohistochemical analysis indicated that some HB-EGF was expressed by vascular SMCs, and HB-EGF released from SMCs has been suggested to function as an autocrine SMC effector (45). However, there seems to be less HB-EGF made by SMCs than by ECs. Immunohistochemical analysis indicated more HB-EGF expression in the EC layer than the SMC layer in developing arterial structures; HB-EGF protein was barely detectable by Western blot under conditions that clearly gave a band for HUVEC-derived HB-EGF (Fig. 2*B*; data not shown) and HASMCs expressed only 0.4% of the HB-EGF mRNA amount expressed by HUVECs in real-time RT-PCR analysis. Thus, ECs are expected to be a more important and quantitatively greater biological source for HB-EGF in regulation of directional SMC chemotaxis than SMCs themselves.

In spite of indirect indications (2, 42, 46), this report is to our knowledge the first in which the significance of HB-EGF and the ErbB signaling system in mediating SMC migration has been experimentally addressed. To analyze this, we tested inhibitors of the HB-EGF signaling pathway for their effects on EC-stimulated SMC migration. A specific HB-EGF inhibitor (CRM 197), a neutralizing anti-HB-EGF antibody, a small molecular weight inhibitor of ErbB1 (PD 153035), and an inhibitory antibody against ErbB2 (Herceptin) all blocked HUVEC medium-stimulated migratory response of HASMCs by 90 to 100%. These findings suggest that inhibiting HB-EGF-stimulated ErbB signaling could also be a way to interfere with EC–SMC interaction during pathological angiogenesis in vivo. Recent reports indicate that some of the clinical anti-tumor effects of the ErbB1 and ErbB2 inhibitors Iressa and Herceptin, respectively, could be explained by anti-angiogenic effects on tumor vasculature (47, 48).

In contrast to HUVEC-stimulated migration of HASMCs, CRM 197 was significantly less potent in blocking BCE-stimulated migration of BASMCs. This was not an obvious outcome of bovine cells being less sensitive to CRM 197, since the ErbB1 inhibitor PD 153035 was also significantly less potent in inhibiting BCE-stimulated migration of BASMCs compared with HUVEC-stimulated migration of HASMCs (data not shown). Bovine cells are known to be sensitive to the toxic variant of CRM 197, diphtheria toxin (E. Mekada, personal communication), indicating that bovine HB-EGF indeed interacts with CRM 197. One could speculate that since BCE-conditioned medium efficiently recruited SMCs whereas BCEs seemed to express less HB-EGF protein than HUVECs (based on analysis with an antibody against mouse HB-EGF), factors other than HB-EGF might play a more important role in BCE-stimulated SMC recruitment compared with HUVECs. Taken together, these findings strongly support a central role for HB-EGF in mediating EC-stimulated recruitment of SMCs, but also indicate that the relative importance of HB-EGF in this signaling may vary between the heterogenic vascular beds. Elucidation of the relative contributions of HB-EGF and other factors, such as of PDGF-B, in the recruitment of SMCs in different vascular structures needs further in vitro and in vivo experiments in which various vessel types and ligands are analyzed simultaneously. For example, no information is currently available about the vascular phenotype of targeted HB-EGF $-/-$ mouse (49).

Mice lacking Ang-1 or Tie2 genes or overexpressing the antagonist Ang-2 have defects in the developing vessels associated with a lack of recruitment of PCs and SMCs (7–9). Since angiopoietins are supposed to signal solely via the EC-specific Tie2 (4), these findings indicate an indirect mechanism in which Ang-1/Tie2 signaling stimulates the production of a soluble SMC chemoattractant, such as PDGF-B, from ECs (2). Mice lacking Ang-1 or Tie2 already have defects in the SMC coverage of large vessels around embryonic day 10, when these structures in PDGF-B- or PDGFR-β-deficient mice still develop normally (5). These reports support the presence of EC-derived SMC chemoattractants other than PDGF-B and suggest that the expression of such a factor could be regulated by angiopoietins. Here we demonstrate that Ang-1 stimulated the expression of HB-EGF in HUVECs. In addition, conditioned medium from AdAng-1 or recombinant Ang-1-treated HUVECs stimulated more HASMC migration than control media, and HB-EGF neutralization significantly blocked the enhanced migration. These findings suggest that endothelial HB-EGF expression is under the regulation of a central effector of vascular maturation, Ang-1, and support a crucial role for HB-EGF in a pathway mediating SMC recruitment by Ang-1. One possible source for Ang-1 in vivo is mesenchymal cells surrounding developing blood vessels (50). This is consistent with the observation that HASMCs used in our experiments expressed considerable amounts of Ang-1 mRNA but significantly less Ang-2 mRNA (2.4% and 0.07% of β-actin mRNA, respectively) when analyzed by real-time RT-PCR and that serum-free conditioned medium from HASMC up-regulated HB-EGF expression in HUVECs (unpublished observations).

The Ang-1/Tie2 signaling system has been suggested to interact with the EGF/ErbB system during the development of the heart. The heart phenotypes of mice deficient in Ang-1, Tie2, NRG-1, ErbB2, and ErbB4 are almost identical, each demonstrating a lack of myocardial trabeculae (7, 8, 20–22). Ang-1 secreted from the myocardial cells and signaling via the Tie2 in endocardial cells has been proposed to reciprocally communicate with NRG-1 expressed in endocardium and signaling via the ErbB2/ErbB4 heterodimer in myocardial cells. Taken together, these observations and the data presented in this paper support a model in which cross-talk between the ErbB and Tie receptor tyrosine kinase subfamilies plays a role in the development and maintenance of several different cardiovascular structures. Tissue specificity in this cross-talk may be achieved by differential expression of the members of the ErbB system, e.g., by NRG-1 signaling via ErbB2/ErbB4 in the heart and by HB-EGF signaling via ErbB1/ErbB2 in blood vascular structures.

Collectively, the results suggest that HB-EGF is the major EGF-like ligand expressed by ECs that participates in the paracrine signaling from ECs to SMCs. The receptors that mediate HB-EGF signaling in SMCs are ErbB1 and ErbB2, indicating that this signaling pathway can be inhibited by available ErbB inhibitor drugs. Furthermore, the finding that Ang-1 up-regulates the capacity of ECs to recruit SMCs in an HB-EGF-dependent manner suggests a novel indirect mechanism by which angiopoietins regulate the maturation of blood vessels.

Drs. Michael Klagsbrun, Eiichiro Nishi, and Mikko Savontaus are acknowledged for valuable comments and discussions. Katri Aarniemi, Pia Kuivas, and Maria Tuominen are acknowledged for excellent technical assistance. This work has been supported by the Academy of Finland, Emil Aaltonen Foundation, Sigrid Juselius Foundation, the Turku

University Central Hospital, the Finnish Cancer Organization, the Turku University Foundation, Ida Montin Foundation, and Aurator Biomed Fund.

REFERENCES

1. Jones, N., Iljin, K., Dumont, D. J., and Alitalo, K. (2001) Tie receptors: new modulators of angiogenic and lymphangiogenic responses. *Nat. Rev. Mol. Cell Biol.* **2,** 257–267
2. Folkman, J., and D'Amore, P. A. (1996) Blood vessel formation: what is its molecular basis? *Cell* **87,** 1153–1155
3. Carmeliet, P. (2000) Mechanisms of angiogenesis and arteriogenesis. *Nat. Med.* **6,** 389–395
4. Yancopoulos, G. D., Davis, S., Gale, N. W., Rudge, J. S., Wiegand, S. J., and Holash, J. (2000) Vascular-specific growth factors and blood vessel formation. *Nature (London)* **407,** 242–248
5. Lindahl, P., Johansson, B. R., Leveen, P., and Betsholtz, C. (1997) Pericyte loss and microaneurysm formation in PDGF-B-deficient mice. *Science* **277,** 242–245
6. Hellström, M., Kalén, M., Lindahl, P., Abramsson, A., and Betsholtz, C. (1999) Role of PDGF-B and PDGFR-beta in recruitment of vascular smooth muscle cells and pericytes during embryonic blood vessel formation in the mouse. *Development* **126,** 3047–3055
7. Sato, T. N., Tozawa, Y., Deutsch, U., Wolburg-Buchholz, K., Fujiwara, Y., Gendron-Maguire, M., Gridley, T., Wolburg, H., Risau, W., and Qin, Y. (1995) Distinct roles of the receptor tyrosine kinases Tie-1 and Tie-2 in blood vessel formation. *Nature (London)* **376,** 70–74
8. Suri, C., Jones, P. F., Patan, S., Bartunkova, S., Maisonpierre, P. C., Davis, S., Sato, T. N., and Yancopoulos, G. D. (1996) Requisite role of angiopoietin-1, a ligand for the TIE2 receptor, during embryonic angiogenesis. *Cell* **87,** 1171–1180
9. Maisonpierre, P. C., Suri, C., Jones, P. F., Bartunkova, S., Wiegand, S. J., Radziejewski, C., Compton, D., McClain, J., Aldrich, T. H., Papadopoulos, N., et al. (1997) Angiopoietin-2, a natural antagonist for Tie2 that disrupts in vivo angiogenesis. *Science* **277,** 55–60
10. Dumont, D. J., Gradwohl, G., Fong, G. H., Puri, M. C., Gertsenstein, M., Auerbach, A., and Breitman, M. L. (1994) Dominant-negative and targeted null mutations in the endothelial receptor tyrosine kinase, tek, reveal a critical role in vasculogenesis of the embryo. *Genes Dev.* **8,** 1897–1909
11. Ullrich, A., Coussens, L., Hayflick, J. S., Dull, T. J., Gray, A., Tam, A. W., Lee, J., Yarden, Y., Libermann, T. A., Schlessinger, J., et al. (1984) Human epidermal growth factor receptor cDNA sequence and aberrant expression of the amplified gene in A431 epidermoid carcinoma cells. *Nature (London)* **309,** 418–425
12. Yamamoto, T., Ikawa, S., Akiyama, T., Semba, K., Nomura, N., Miyajima, N., Saito, T., and Toyoshima, K. (1986) Similarity of protein encoded by the human c-erb-B-2 gene to epidermal growth factor receptor. *Nature (London)* **319,** 230–234
13. Kraus, M. H., Issing, W., Miki, T., Popescu, N. C., and Aaronson, S. A. (1989) Isolation and characterization of ERBB3, a third member of the ERBB/epidermal growth factor receptor family: evidence for overexpression in a subset of human mammary tumors. *Proc. Natl. Acad. Sci. USA* **86,** 9193–9197
14. Junttila, T., Sundvall, M., Määttä, J. A., and Elenius, K. (2001) ErbB4 and its isoforms. Selective regulation of growth factor responses by naturally occurring receptor variants. *Trends Cardiovasc. Med.* **10,** 304–310
15. Plowman, G. D., Culouscou, J. M., Whitney, G. S., Green, J. M., Carlton, G. W., Foy, L., Neubauer, M. G., and Shoyab, M. (1993) Ligand-specific activation of HER4/p180erbB4, a fourth member of the epidermal growth factor receptor family. *Proc. Natl. Acad. Sci. USA* **90,** 1746–1750
16. Riese, D. J., and Stern, D. F. (1998) Specificity within the EGF family/ErbB receptor family signaling network. *Bioessays* **20,** 41–48
17. Yarden, Y., and Sliwkowski, M. X. (2001) Untangling the ErbB signalling network. *Nat. Rev. Mol. Cell Biol.* **2,** 127–137
18. Strachan, L., Murison, J. G., Prestidge, R. L., Sleeman, M. A., Watson, J. D., and Kumble, K. D. (2001) Cloning and biological activity of epigen, a novel member of the EGF superfamily. *J. Biol. Chem.* **276,** 18265–18271
19. Olayioye, M. A., Neve, R. M., Lane, H. A., and Hynes, N. E. (2000) The ErbB signaling network: receptor heterodimerization in development and cancer. *EMBO J.* **19,** 3159–3167
20. Meyer, D., and Birchmeier, C. (1995) Multiple essential functions of neuregulin in development. *Nature (London)* **378,** 386–390
21. Gassmann, M., Casagranda, F., Orioli, D., Simon, H., Lai, C., Klein, R., and Lemke, G. (1995) Aberrant neural and cardiac development in mice lacking the ErbB4 neuregulin receptor. *Nature (London)* **378,** 390–394
22. Lee, K. F., Simon, H., Chen, H., Bates, B., Hung, M. C., and Hauser, C. (1995) Requirement for neuregulin receptor erbB2 in neural and cardiac development. *Nature (London)* **378,** 394–398
23. Higashiyama, S., Horikawa, M., Yamada, K., Ichino, N., Nakano, N., Nakagawa, T., Miyagawa, J., Matsushita, N., Nagatsu, T., Taniguchi, N., et al. (1997) A novel brain-derived member of the epidermal growth factor family that interacts with ErbB3 and ErbB4. *J. Biochem.* **122,** 675–680
24. Jones, N., Master, Z., Jones, J., Bouchard, D., Gunji, Y., Sasaki, H., Daly, R., Alitalo, K., and Dumont, D. J. (1999) Identification of Tek/Tie2 binding partners. Binding to a multifunctional docking site mediates cell survival and migration. *J. Biol. Chem.* **274,** 30896–30905
25. Nykanen, A. I., Krebs, R., Saaristo, A., Turunen, P., Alitalo, K., Yla-Herttuala, S., Koskinen, P. K., and Lemstrom, K. B. (2003) Angiopoietin-1 protects against the development of cardiac allograft arteriosclerosis. *Circulation* **107,** 1308–1314
26. Laitinen, M., Makinen, K., Manninen, H., Matsi, P., Kossila, M., Agrawal, R. S., Pakkanen, T., Luoma, J. S., Viita, H., Hartikainen, J., et al. (1998) Adenovirus-mediated gene transfer to lower limb artery of patients with chronic critical leg ischemia. *Hum. Gene Ther.* **9,** 1481–1486
27. Naglich, J. G., Metherall, J. E., Russell, D. W., and Eidels, L. (1992) Expression cloning of a diphtheria toxin receptor: identity with a heparin-binding EGF-like growth factor precursor. *Cell* **69,** 1051–1061
28. Mitamura, T., Higashiyama, S., Taniguchi, N., Klagsbrun, M., and Mekada, E. (1995) Diphtheria toxin binds to the epidermal growth factor (EGF)-like domain of human heparin-binding EGF-like growth factor/diphtheria toxin receptor and inhibits specifically its mitogenic activity. *J. Biol. Chem.* **270,** 1015–1019
29. Jaffe, E. A., Nachman, R. L., Becker, C. G., and Minick, C. R. (1973) Culture of human endothelial cells derived from umbilical veins. Identification by morphologic and immunologic criteria. *J. Clin. Invest.* **52,** 2745–2756
30. Järveläinen, H. T., Kinsella, M. G., Wight, T. N., and Sandell, L. J. (1991) Differential expression of small chondroitin/dermatan sulfate proteoglycans, PG-I/biglycan and PG-II/decorin, by vascular smooth muscle and endothelial cells in culture. *J. Biol. Chem.* **266,** 23274–23281
31. Boyden, S. (1962) The chemotactic effect of mixtures of antibody and antigen on polymorphonuclear leukocytes. *J. Exp. Med.* **115,** 453–466
32. Kainulainen, V., Sundvall, M., Määttä, J. A., Santiestevan, E., Klagsbrun, M., and Elenius, K. (2000) A natural ErbB4 isoform that does not activate phosphoinositide 3-kinase mediates proliferation but not survival or chemotaxis. *J. Biol. Chem.* **275,** 8641–8649
33. Higashiyama, S., Abraham, J. A., Miller, J., Fiddes, J. C., and Klagsbrun, M. (1991) A heparin-binding growth factor secreted by macrophage-like cells that is related to EGF. *Science* **251,** 936–939
34. Iruela-Arispe, M. L., Hasselaar, P., and Sage, H. (1991) Differential expression of extracellular proteins is correlated with angiogenesis in vitro. *Lab. Invest.* **64,** 174–186
35. Zhang, K., Sun, J., Liu, N., Wen, D., Chang, D., Thomason, A., and Yoshinaga, S. K. (1996) Transformation of NIH 3T3 cells by HER3 or HER4 receptors requires the presence of HER1 or HER2. *J. Biol. Chem.* **271,** 3884–3890
36. Beerli, R. R., Graus Porta, D., Woods Cook, K., Chen, X., Yarden, Y., and Hynes, N. E. (1995) Neu differentiation factor activation of ErbB-3 and ErbB-4 is cell specific and displays a differential requirement for ErbB-2. *Mol. Cell. Biol.* **15,** 6496–6505

37. Pierce, J. H., Ruggiero, M., Fleming, T. P., Di Fiore, P. P., Greenberger, J. S., Varticovski, L., Schlessinger, J., Rovera, G., and Aaronson, S. A. (1988) Signal transduction through the EGF receptor transfected in IL-3-dependent hematopoietic cells. *Science* **239,** 628–631
38. Zhu, M., Madigan, M. C., van Driel, D., Maslim, J., Billson, F. A., Provis, J. M., and Penfold, P. L. (2000) The human hyaloid system: cell death and vascular regression. *Exp. Eye Res.* **70,** 767–776
39. Riese, D. J., Kim, E. D., Elenius, K., Buckley, S., Klagsbrun, M., Plowman, G. D., and Stern, D. F. (1996) The epidermal growth factor receptor couples transforming growth factor-alpha, heparin-binding epidermal growth factor-like factor, and amphiregulin to Neu, ErbB-3, and ErbB-4. *J. Biol. Chem.* **271,** 20047–20052
40. Russell, K. S., Stern, D. F., Polverini, P. J., and Bender, J. R. (1999) Neuregulin activation of ErbB receptors in vascular endothelium leads to angiogenesis. *Am. J. Physiol.* **277,** H2205–H2211
41. Yoshizumi, M., Kourembanas, S., Temizer, D. H., Cambria, R. P., Quertermous, T., and Lee, M. E. (1992) Tumor necrosis factor increases transcription of the heparin-binding epidermal growth factor-like growth factor gene in vascular endothelial cells. *J. Biol. Chem.* **267,** 9467–9469
42. Arkonac, B. M., Foster, L. C., Sibinga, N. E., Patterson, C., Lai, K., Tsai, J. C., Lee, M. E., Perrella, M. A., and Haber, E. (1998) Vascular endothelial growth factor induces heparin-binding epidermal growth factor-like growth factor in vascular endothelial cells. *J. Biol. Chem.* **273,** 4400–4405
43. Raab, G., and Klagsbrun, M. (1997) Heparin-binding EGF-like growth factor. *Biochim. Biophys. Acta* **1333,** F179–F199
44. Higashiyama, S., Abraham, J. A., and Klagsbrun, M. (1993) Heparin-binding EGF-like growth factor stimulation of smooth muscle cell migration: dependence on interactions with cell surface heparan sulfate. *J. Cell Biol.* **122,** 933–940
45. Higashiyama, S., Abraham, J. A., and Klagsbrun, M. (1994) Heparin-binding EGF-like growth factor synthesis by smooth muscle cells. *Horm. Res.* **42,** 9–13
46. Abramovitch, R., Neeman, M., Reich, R., Stein, I., Keshet, E., Abraham, J., Solomon, A., and Marikovsky, M. (1998) Intercellular communication between vascular smooth muscle and endothelial cells mediated by heparin-binding epidermal growth factor-like growth factor and vascular endothelial growth factor. *FEBS Lett.* **425,** 441–447
47. Ciardiello, F., Caputo, R., Bianco, R., Damiano, V., Fontanini, G., Cuccato, S., De Placido, S., Bianco, A. R., and Tortora, G. (2001) Inhibition of growth factor production and angiogenesis in human cancer cells by ZD1839 (Iressa), a selective epidermal growth factor receptor tyrosine kinase inhibitor. *Clin. Cancer Res.* **7,** 1459–1465
48. Izumi, Y., Xu, L., di Tomaso, E., Fukumura, D., and Jain, R. K. (2002) Tumour biology: Herceptin acts as an anti-angiogenic cocktail. *Nature (London)* **416,** 279–280
49. Iwamoto, R., Yamazaki, S., Asakura, M., Takashima, S., Hasuwa, H., Miyado, K., Adachi, S., Kitakaze, M., Hashimoto, K., Raab, G., et al. (2003) Heparin-binding EGF-like growth factor and ErbB signaling is essential for heart function. *Proc. Natl. Acad. Sci. USA* **100,** 3221–3226
50. Davis, S., Aldrich, T. H., Jones, P. F., Acheson, A., Compton, D. L., Jain, V., Ryan, T. E., Bruno, J., Radziejewski, C., Maisonpierre, P. C., et al. (1996) Isolation of angiopoietin-1, a ligand for the TIE2 receptor, by secretion-trap expression cloning. *Cell* **87,** 1161–1169

Received for publication October 23, 2002.
Accepted for publication April 22, 2003.

MOLECULAR AND CELLULAR BIOLOGY, Jan. 2003, p. 55–61 Vol. 23, No. 1
0270-7306/03/$08.00+0 DOI: 10.1128/MCB.23.1.55–61.2003

Phenotypic Analysis of Meltrin α (ADAM12)-Deficient Mice: Involvement of Meltrin α in Adipogenesis and Myogenesis

Tomohiro Kurisaki,[1] Aki Masuda,[1] Katsuko Sudo,[2] Junko Sakagami,[2] Shigeki Higashiyama,[3] Yoichi Matsuda,[4,5] Akira Nagabukuro,[5] Atsushi Tsuji,[5] Yoichi Nabeshima,[6] Masahide Asano,[7] Yoichiro Iwakura,[2] and Atsuko Sehara-Fujisawa[1]*

Field of Growth Regulation, Institute for Frontier Medical Sciences, Kyoto University, Kyoto 606-8507,[1] Center for Experimental Medicine, Institute of Medical Science, University of Tokyo, Tokyo 108-8639,[2] Department of Medical Biochemistry, Ehime University School of Medicine, Ehime 791-0295,[3] Laboratory of Animal Cytogenetics, Center for Advanced Science and Technology, Hokkaido University, Sapporo 060-0810,[4] Laboratory of Animal Genetics, Graduate School of Bioagricultural Science, Nagoya University, Chikusa-ku, Nagoya 464-8601,[5] Department of Pathology and Tumor Biology, Kyoto University Graduate School of Medicine, Kyoto 606-8501,[6] and Institute for Experimental Animals, School of Medicine, Kanazawa University, Kanazawa 920-8640,[7] Japan

Received 29 May 2002/Returned for modification 28 August 2002/Accepted 7 October 2002

Meltrin α (ADAM12) is a metalloprotease-disintegrin whose specific expression patterns during development suggest that it is involved in myogenesis and the development of other organs. To determine the roles Meltrin α plays in vivo, we generated Meltrin α-deficient mice by gene targeting. Although the number of homozygous embryos are close to the expected Mendelian ratio at embryonic days 17 to 18, ca. 30% of the null pups born die before weaning, mostly within 1 week of birth. The viable homozygous mutants appear normal and are fertile. Most of the muscles in the homozygous mutants appear normal, and regeneration in experimentally damaged skeletal muscle is unimpeded. In some Meltrin α-deficient pups, the interscapular brown adipose tissue is reduced, although the penetrance of this phenotype is low. Impaired formation of the neck and interscapular muscles is also seen in some homozygotes. These observations suggest Meltrin α may be involved in regulating adipogenesis and myogenesis through a linked developmental pathway. Heparin-binding epidermal growth factor-like growth factor (HB-EGF) is a candidate substrate of Meltrin α, and we found that TPA (12-*O*-tetradecanoylphorbol-13-acetate)-induced ectodomain shedding of HB-EGF is markedly reduced in embryonic fibroblasts prepared from Meltrin α-deficient mice. We also report here the chromosomal locations of Meltrin α in the mouse and rat.

Meltrin α is a metalloprotease-disintegrin that belongs to the ADAM (for "a disintegrin and metalloprotease") family. To date, more than 30 ADAMs in worms, flies, rodents, primates, and humans have been identified (3, 44). ADAMs are thought to be involved in various biological functions, including fertilization, myogenesis, neurogenesis, and the development of various epithelial tissues (3, 30, 35). For example, Fertilin α and Fertilin β, which were the first identified mammalian ADAMs, play important roles in fertilization (4, 8). Another example is Kuzbanian (ADAM10), which is known to be involved in neurogenesis by regulating Notch signaling (18, 28, 31, 40). Some ADAMs are catalytically active metalloproteases and participate in the proteolytic processing of the extracellular domains of membrane-anchored proteins (44). For example, TACE (ADAM17) was initially identified as the protease responsible for the processing of tumor necrosis factor alpha (2, 23). Studies on TACE-null mice then revealed that TACE is involved in the processing of the extracellular domains of several membrane-anchored proteins, including the tumor necrosis factor p75 receptor, the adhesion molecule L-selectin, the amyloid precursor protein, and transforming growth factor α (7). Another example is Meltrin β (ADAM19), which has been shown to be involved in the in vitro processing of Neuregulin β, another membrane-anchored growth factor (37). Other studies suggest that ADAMs are also involved in cell-cell or cell-extracellular matrix interactions through their interaction with integrins (6, 10, 27, 48) or proteoglycans (15).

We previously showed that Meltrin α promotes myotube formation in vitro (45). Furthermore, Meltrin α is specifically expressed in the muscles during the neonatal stages and in the bones of both neonates and adults. In addition, during embryogenesis, Meltrin α mRNA was found in the mesenchymes of the lungs and the intestines and in the placenta (17), which suggests that Meltrin α is involved in organogenesis. Based on its amino acid sequence, the metalloprotease domain of Meltrin α is presumed to be catalytically active. Supporting this notion are the reports that it has proteolytic activity in vitro. For example, human Meltrin α interacts with insulin-like growth factor-binding protein 3 (IGFBP-3) (36) and cleaves it in vitro (19). Furthermore, Meltrin α has also recently been implicated to act as a sheddase with heparin-binding epidermal growth factor-like growth factor (HB-EGF) (1). To further determine the function of Meltrin α in mouse development, we generated and analyzed Meltrin α gene-targeted mice.

* Corresponding author. Mailing address: Field of Growth Regulation, Institute for Frontier Medical Sciences, Kyoto University, Kyoto, 606-8507, Japan. Phone: 81-75-751-3826. Fax: 81-75-751-4642. E-mail: asehara@frontier.kyoto-u.ac.jp.

Materials and Methods

Materials. Chemicals were purchased from Sigma (St. Louis, Mo.) and nacalai tesque (Kyoto, Japan). Restriction enzymes and reagents for molecular biology were purchased from TaKaRa (Kyoto, Japan) and Toyobo (Osaka, Japan) unless otherwise indicated.

Construction of Meltrin α gene-targeting vector. The Meltrin α gene isolated from a 129/SvJ genomic library (Stratagene) was used to construct the targeting vector. The PGKneobpA cassette from pPGKneobpA (39) was inserted between a 5′ homologous region (*Xho*I-*Bam*HI [9 kb]) and a 3′ homologous region (*Sac*II-*Sac*I [1.5 kb]). The DT-A cassette (46) was ligated at the 3′ end of the targeting vector for negative selection. In this construct, the exon containing the initiation codon was deleted.

Generation of Meltrin $\alpha^{-/-}$ mice. The linearized targeting vector (20 μg) was electroporated (250 V, 500 μF) into 10^7 R1 embryonic stem (ES) cells (26) and selected with 180 μg (active form) of G418 (Gibco-BRL)/ml for 7 to 10 days. Homologous recombinants were selected by PCR and confirmed by Southern blot analysis. The forward primer in the PGKneobpA cassette was 5′-TGGAT GTGGAATGTGTGCGAGG-3′, and the reverse primer outside the targeting vector was 5′-TTCCATTGCTCAGCGGTGCTGTC-3′. PCR was performed with LA *Taq* DNA polymerase (TaKaRa, Kyoto, Japan) for 30 cycles at 98°C for 20 s and at 68°C for 10 min in a volume of 50 μl. Two ES clones that yielded hybridization bands of the correct size gave rise to germ line chimeras by the aggregation method (26). The resulting chimeras were backcrossed to C57BL/6J, and N_8 mice were used in the following experiments. The genotypes were determined by either PCR (for embryos) or Southern blot analysis. Genotyping PCR was performed as follows: the primer set in the PGKneobpA cassette (5′-TGGAGAGGCTATTCGGCTATGACTGGG-3′ and 5′-ATGCAGCCGCC GCATTGCAT-3′) was used to detect targeted alleles. PCR was performed with Ampli*Taq* Gold DNA polymerase (PE Applied Biosystems) for 40 cycles at 96°C for 15 s and at 70°C for 30 s in a volume of 15 μl. The primer set in the exon containing the initiation codon (5′-GCGCTCTGCCATTGTCGCCG-3′ and 5′-GGCAGACTCAGGGCAGTAGGACTTCCC-3′) was used to detect wild-type alleles. PCR conditions used were the same as those for the targeted allele detection PCR, except that the annealing and extension temperatures used were both 64°C. Southern blot and reverse transcription-PCR (RT-PCR) analyses were performed as follows: genomic DNA from ES cells or mouse tail was digested with restriction enzymes, electrophoresed through a 0.8% agarose gel and transferred to Hybond-XL membrane (Amersham Pharmacia Biotech). Hybridization was performed according to standard methods (33) with a ^{32}P-labeled DNA probe made by using a Megaprime DNA labeling kit (Amersham Pharmacia Biotech). A 1.2-kb *Sac*I-*Hin*dIII fragment immediately downstream of the 3′ end of the 3′ homology region was used as the probe. RT-PCR was performed as follows. mRNA was extracted from embryos by using a QuickPrep Micro mRNA purification kit (Amersham Pharmacia Biotech). cDNA was synthesized from the mRNA by using the SuperScript first-strand synthesis system (Invitrogen). PCR was carried out with Ampli*Taq* Gold DNA polymerase. The primers used to detect mRNA of Meltrin α were 5′-GATGACCAAGTACGTAGAGC TGG-3′ and 5′-TCATGGAGCCTGGTGAATGGG-3′ (for the metalloprotease domain), 5′-GAGTGTGACTGCGGAGAACCGGAGGAA-3′ and 5′-ATTTT CCCACACTTGGCATCTCTCA-3′ (for the disintegrin domain), 5′-GTCAAG GTGGTGCAAGCCGA-3′ and 5′-TGATGGGACCACTGTCTGTGC-3′ (for the cysteine-rich domain), and 5′-GACGTTGATGCGGCTGCTGTTC-3′ and 5′-GCGTCGAGGGGCCTGCTGATG-3′ (for the cytoplasmic domain). The glyceradehyde-3-phosphate dehydrogenase 0.45-kb control amplimer set (Clontech) was used as a positive control. Mice were maintained under specific-pathogen-free conditions in environmentally controlled clean rooms at the Laboratory Animal Research Center, Institute of Medical Science, University of Tokyo, the Animal Facility, Tokyo Institute of Medical Science, and at the Institute for Frontier Medical Sciences, Kyoto University. The experiments were conducted according to institutional ethical guidelines for animal experimentation and safety guidelines for gene manipulation experiments.

Histology. Embryos were fixed in 4% paraformaldehyde–phosphate-buffered saline (PBS). Fixed samples were dehydrated by sequentially increased ethanol concentrations, cleared in xylene, and then embedded in paraffin. The embedded samples were sectioned into 4.5-μm-thick slices and stained with hematoxylin and eosin (HE).

In situ hybridization. In situ hybridization was performed with digoxigenin-labeled antisense and sense riboprobes prepared by in vitro transcription according to the manufacturer's protocol (Roche Molecular Biochemicals). The antisense probe for Meltrin α consisted of two 1.3-kb fragments that spanned nucleotides 93 to 1417 and nucleotides 1997 to 3338.

Mouse embryonic fibroblasts. Embryonic day 13.5 (E13.5) embryos from Meltrin α knockout and wild-type mice were used to generate mouse embryonic fibroblasts (14). Briefly, the head, limbs, and viscera were removed from the embryos, and the carcasses were minced and then trypsinized in 0.05% trypsin 0.02% EDTA in PBS for 10 min at 37°C. Cells were collected and grown in 10% fetal calf serum in Dulbecco's modified Eagle medium (DMEM).

HB-EGF ectodomain shedding assay. Embryonic fibroblast cells prepared from wild-type and knockout mice were seeded in 6-cm dishes at a density of 2 × 10^5 cells/dish and cultured for 48 h with DMEM–10% fetal calf serum. Cells were incubated for 1 h at 37°C with 100 nM TPA (12-*O*-tetradecanoylphorbol-13-acetate). Cells were washed three times with ice-cold Hanks buffer and biotinylated with 0.1 mg of sulfo-NHS-biotin/ml in 50 mM HEPES (pH 7.5)–0.15 M NaCl for 10 min on ice. Excess reagent was quenched and removed by washing with ice-cold DMEM-fetal calf serum. Cells were lysed with a buffer containing 1% Triton X-100, 1 mM EDTA, 1 mM (*p*-amidinophenyl)methanesulfonyl fluoride HCl, 1 μg of aprotinin/ml, and 0.4 M NaCl in 20 mM HEPES (pH 7.2). After centrifugation of the lysates at 15,000 rpm for 10 min, supernatants were collected and incubated with 2 μg of HB-EGF antibody H1 for 2 h at 4°C, followed by incubation with 10 μl of protein G-Sepharose (50% suspension) for 2 h at 4°C. After centrifugation of the mixes, the pellets were analyzed by sodium dodecyl sulfate-polyacrylamide gel electrophoresis and Western blotting as described previously (13).

FISH. The chromosomal assignment of the murine and rat Meltrin α genes was made by direct R-banding fluorescence in situ hybridization (FISH) with a mouse cDNA fragment as a probe (nucleotides 93 to 1417). Chromosome preparation and FISH detection were performed as described previously (21, 22).

RESULTS

Generation of Meltrin α-deficient mice. Meltrin α-deficient mice were generated by homologous recombination. The exon containing the initiation codon was replaced with the neomycin-resistant cassette (Fig. 1a). Homologous recombination was confirmed by Southern blot analysis (Fig. 1b). The hetero- and homozygotes had a normal appearance, and the males and females were both fertile. To confirm that homozygotes do not express Meltrin α, RT-PCR was performed. PCR primer sets for each of the metalloprotease, disintegrin, cysteine-rich, and cytoplasmic domains of Meltrin α did not detect Meltrin α mRNA in the homozygous mutant embryos (E14.5) (Fig. 1c). Despite the normal appearance of the null homozygotes, the number of these homozygotes at weaning was lower than the expected Mendelian ratio in the heterozygous crosses, although the ratio of wild types, heterozygotes, and homozygotes was Mendelian prior to birth (E16.5 to E18.5) (Table 1). That is, during the perinatal period, especially P1-2, the number of homozygous mutants declined, with ca. 30% of the homozygotes dying before weaning. The cause of death is still unclear. Similar results were observed for both of our lines of Meltrin α-deficient mice, which were obtained from independent ES clones.

Histological analysis of Meltrin $\alpha^{-/-}$ embryos. The Meltrin α-deficient mice appeared grossly normal at weaning. However, detailed anatomical analysis of neonatal mice revealed that the interscapular brown adipose tissue (BAT) was reduced in ca. 30% of the Meltrin α-deficient mice (Fig. 2). Although the number and morphology of the adipose lobes were similar to those of wild-type mice, the lobes were significantly smaller. Some of the homozygotes exhibited looser condensation of adipocytes than the wild-type or heterozygous littermates at ca. E16.5, probably due to the lower cell number (data not shown). In addition, some of the perinatal and newborn homozygotes (E17.5-P1) showed impaired formation of the neck and interscapular muscles (Fig. 2f). Although these muscles occupy

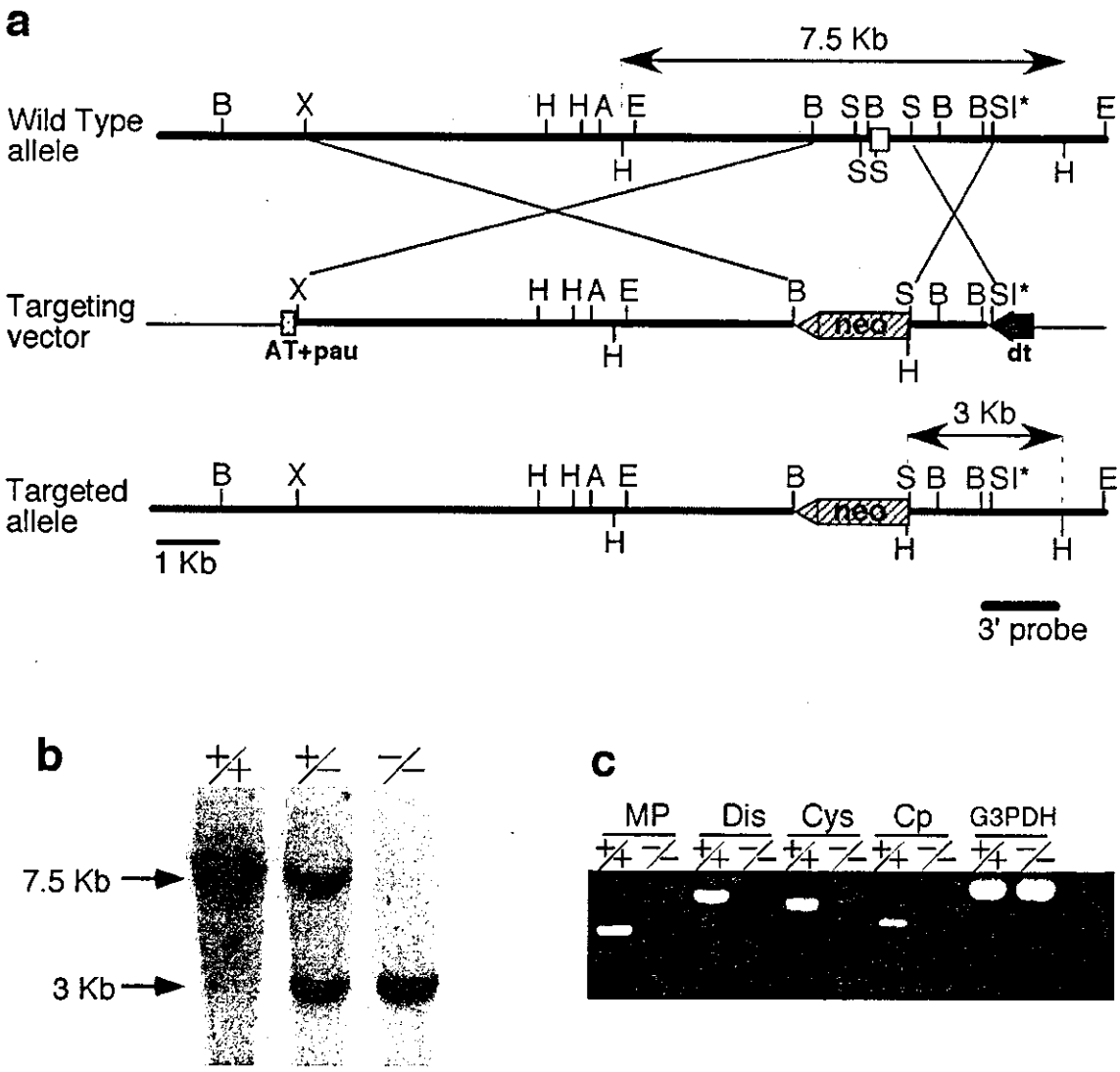

FIG. 1. Generation of Meltrin α-deficient mice. (a) Targeted disruption of the Meltrin α gene. Exon 1 containing the first methionine codon (open box) was replaced by a neocassette. Neo (hatched box) is the neomycin resistance gene, AT+pau (dotted box) indicates the AT-rich RNA polymerase II destabilizing signal and pausing signal, and DT (closed box) is the diphtheria toxin A fragment cassette. The 3′ probe represents the position of the external probe used for Southern blot analysis, and the expected *Hin*dIII fragments are indicated by arrows. Abbreviations: B, *Bam*HI; X, *Xho*I; H, *Hin*dIII; A, *Asp*718; E, *Eco*RI; S, *Sac*II; SI, *Sac*I. The asterisk indicates that the *Sac*I sites in the targeting vector are not unique. (b) Southern blot analysis of mouse tail genomic DNA. The expected DNA fragments for the targeted allele and the wild-type allele are 3 and 7 kb, respectively. +/+, wild-type; +/−, heterozygote; −/−, homozygote. (c) RT-PCR analysis of mRNA from embryonic fibroblasts isolated from E13.5 embryos. MP, primer detecting the metalloprotease domain; Dis, primer detecting the disintegrin domain; Cys, primer detecting the cysteine-rich domain; Cp, primer detecting the cytoplasmic domain. +/−, heterozygote; −/−, homozygote.

areas between the bone and skin that are similar in size to that in the wild type or heterozygotes, the muscle fibers close to the adipose tissues were found not to be as tightly packed in some homozygotes as in the non-null littermates. Although the number of homozygous neonates with impaired BAT or interscapular muscle formation was low (ca. 30%), such defects were never observed in wild-type neonates. However, at 8 weeks of age, all homozygous mice had normal-sized BATs, although some of the interscapular muscles remained slightly reduced in size (data not shown). Since it was not possible to monitor individual mice throughout development, it is not clear

TABLE 1. Genotypic analysis of mice from intercrosses[a]

Mating (female vs male)	Age	No. (%) of mice with genotype:		
		+/+	+/−	−/−
+/− vs +/−	3 wk	66 (30.8)	101 (47.2)	47 (22.0)
	P1-P2	51 (29.0)	92 (52.3)	33 (18.8)
	E16.5-E18.5	25 (23.6)	46 (43.4)	35 (33.0)
+/− vs −/−	3 wk		80 (58.4)	57 (41.6)[b]

[a] +/+, wild type; +/−, heterozygote; −/−, homozygote.
[b] $P < 0.03$.

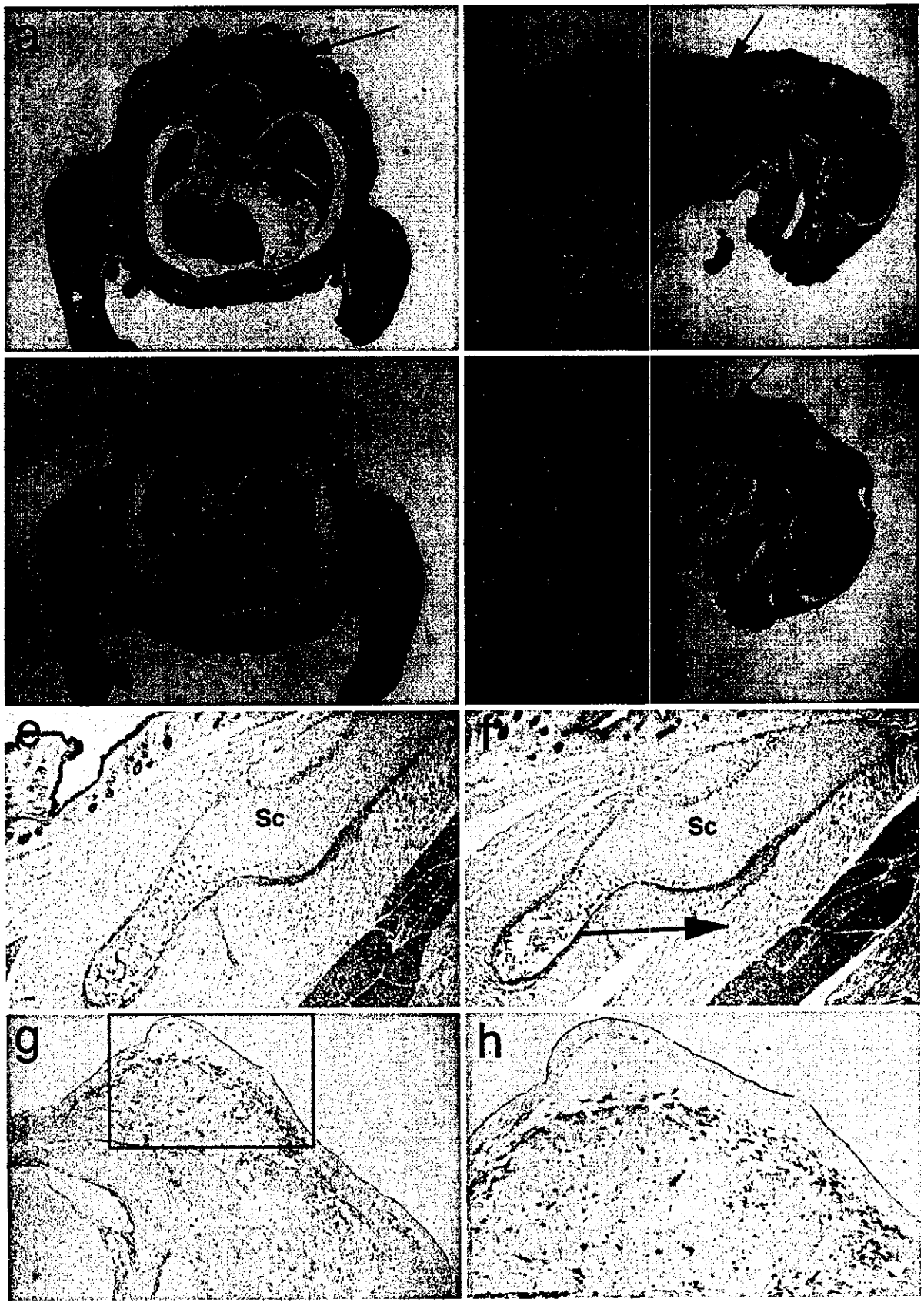
e
Sc
f
Sc
g
h

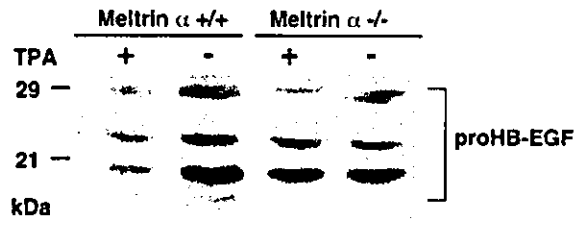

FIG. 3. HB-EGF ectodomain shedding assay. Detection of surface proHB-EGF in mouse embryonic fibroblasts treated with or without TPA. The multiple bands of proHB-EGF are derived from various N-terminal truncations and heterogeneous glycosylations.

whether the size of the BAT recovers after birth or whether mutants with small BATs die.

Muscle regeneration in Meltrin-α-deficient mice. Meltrin-α is activated both in vitro and in vivo during the differentiation of muscle satellite cells (5). Thus, we evaluated the effect Meltrin-α deficiency has on muscle regeneration. When the anterior tibial muscles of adult Meltrin α-deficient mice were experimentally damaged by cardiotoxin treatment, muscle regeneration comparable to that of wild-type mice was observed (data not shown). When we crossed Meltrin α-deficient mice with *mdx* mice, which are muscular dystrophy mutants that show enhanced muscle degeneration and muscle regeneration (9, 41), no enhancement of muscle degeneration or decreased regeneration was observed in the Meltrin-α *mdx* double mutants (data not shown).

Expression of Meltrin α in the BAT-forming region during embryogenesis. In situ hybridization was performed to analyze the expression pattern of Meltrin α during BAT development in the heterozygotes. At E14.5, Meltrin α transcripts were detected in mesenchymal cells in the BAT-forming region beneath the skin (Fig. 2g and h). These Meltrin-α-expressing mesenchymal cells extended to the region of the developing neck muscles adjacent to the BAT tissues, suggesting that these Meltrin α-positive mesenchymal cells are involved in the embryonic development of BAT and adjacent muscle tissues.

HB-EGF ectodomain shedding. Recent studies with metalloprotease inhibitors have implicated metalloproteases in the ectodomain shedding of HB-EGF (1). Therefore, we examined whether Meltrin α can act as a sheddase of HB-EGF in mouse embryonic fibroblasts prepared from E13.5 Meltrin α-deficient or wild-type embryos. Expression of Meltrin α in embryonic fibroblasts was confirmed by RT-PCR (Fig. 1c). Endogenous HB-EGF was detected by cell surface biotinylation, immunoprecipitation, and Western blotting. HB-EGF shedding was evaluated in untreated cells and in TPA-treated cells (Fig. 3). In wild-type embryonic fibroblasts, TPA induced the processing of proHB-EGF (the membrane-anchored form), resulting in the loss of the cell surface proHB-EGF. In contrast, TPA did not induce processing of proHB-EGF in Meltrin α-deficient embryonic fibroblasts. This suggests that Meltrin α contributes to the ectodomain shedding of HB-EGF.

Chromosomal mapping of the murine and rat meltrin α genes. The chromosomal locations of the murine and rat meltrin α genes were determined by direct R-banding FISH with a murine cDNA fragment as a probe (Fig. 4). The Meltrin α genes were localized to the F3 distal −F4 band of mouse chromosome 7 and the q43 proximal band of rat chromosome 1. Conserved linkage homology between these species has been identified in these areas (20, 21, 34, 38, 47). To date, suggestive mutations have not been mapped to Meltrin α. We attempted to linkage map the Meltrin α gene by interspecific backcross analysis with progeny derived from the mating of (C57BL6 3 *Mus spretus*)F_1 × *M. spretus* mice. However, this attempt failed because of the presence of an additional Meltrin α-like gene in *M. spretus* chromosome 2.

DISCUSSION

Meltrin α (ADAM12) was originally cloned from myogenic cells. Its expression pattern suggests that it is involved in various organogenic processes, particularly myogenesis (12, 17, 45). In the present study, we examined the function of Meltrin α during mouse development by generating mice lacking the Meltrin α gene. Unexpectedly, no major morphological abnormalities were observed in Meltrin $\alpha^{-/-}$ mice, and the homozygous mutants were viable and fertile. However, ca. 30% of homozygotes did die within 1 week of birth. The cause of death is unknown. In addition, some homozygous mutants showed impaired formation of interscapular BAT (E17.5-P1).

Mammals have two types of adipose tissue, namely, white adipose tissue (WAT) and BAT (32). Although WAT stores excess energy as triglycerides and releases free fatty acids in response to energy requirements, BAT dissipates energy in the form of heat through the uncoupling of oxidative phosphorylation. It functions as a thermogenerator to maintain the body temperature and protects against obesity. Thus, the impaired formation of BAT can cause hypothermia in neonates. Parents sometimes do not nurse neonates with low body temperatures, which might explain the semilethality of the homozygous mutant neonates. Nevertheless, all surviving adult homozygous mutants had apparently normal BAT and WAT (perigonadal).

It is noteworthy that some Meltrin α-deficient mice also show hypotrophy of muscles adjacent to BAT and that others show a reduction of both tissues. In vitro studies have revealed that both muscle and fat cells can be induced from pluripotent stem cell lines or marrow-derived stromal cells (29, 42). Although the identity and mechanisms of differentiation of such presumptive mesenchymal precursor cells remains unknown, the embryonic expression of Meltrin α and the effect of its absence on BAT and adjacent muscle formation shown in the present study support the idea that the development of these tissues are intimately related. Furthermore, recent studies

FIG. 2. Histological analysis of Meltrin $\alpha^{-/-}$ embryos. Heterozygous (a, b, and e) and homozygous (c, d, and f) neonates (P1) were fixed, embedded in paraffin, sectioned, and stained with HE. The frontal section (a and c) and saggital section (b and d) are shown. BAT is indicated by arrows in panels a to d. The arrow in panel f shows impaired muscle development. Sc, scapular bone; B, BAT. (g and h) The expression of Meltrin α mRNA in heterozygous embryos was detected by in situ hybridization. At E14.5, Meltrin α is expressed in bones, muscles, and the peripheral region of condensing interscapular mesenchymal cells. (Panel h shows an enlarged region of panel g [boxed].)

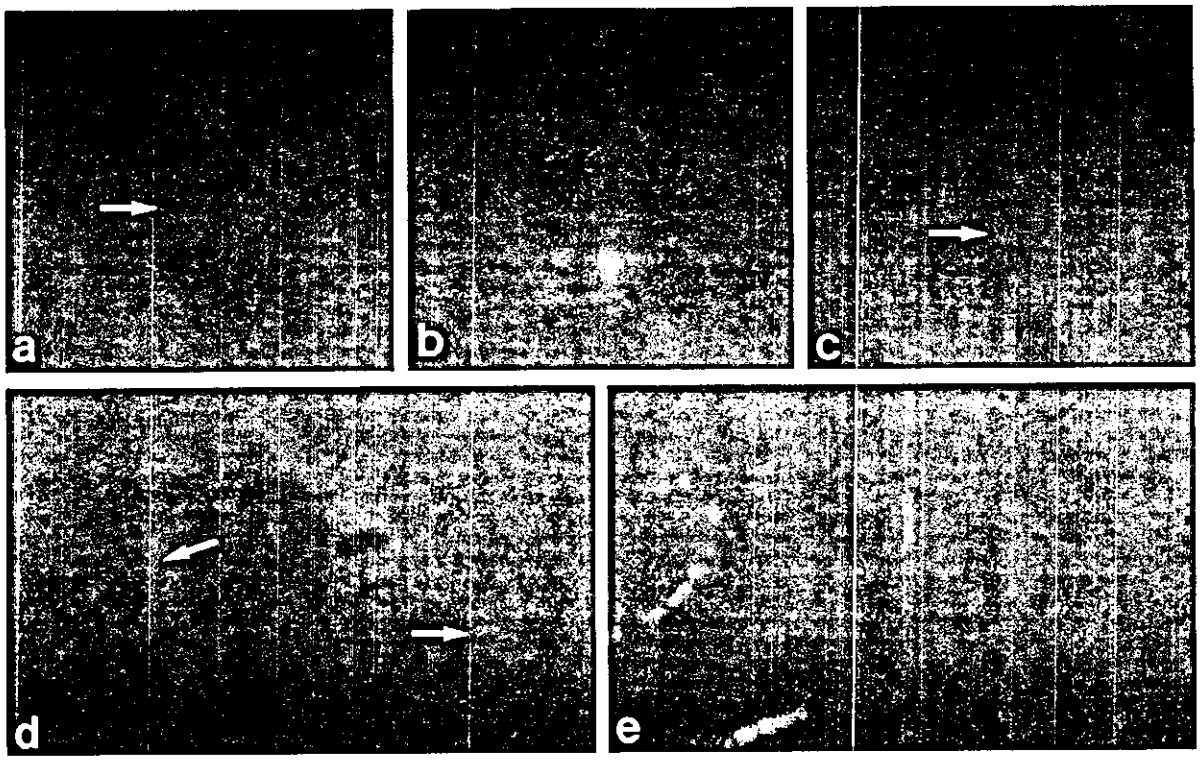

FIG. 4. Chromosomal localization of the Meltrin α gene. Chromosomal localization of the Meltrin α gene on R-banded murine (a to c) and rat (d and e) chromosomes. The chromosomal locations of the murine and rat Meltrin α genes were determined by using a murine cDNA fragment as a biotinylated probe. The hybridization signals are indicated by arrows. The signals are localized to murine chromosome 7F3 distal −F4 and to the rat chromosome 1q43 (proximal). The metaphase spreads were photographed with Nikon B-2A (a, c, and d) and UV-2A (b and e) filters. R-band and G-band patterns are demonstrated in panels a, c, and d and in panels b and e, respectively.

demonstrated that transgenic mice overexpressing Meltrin α have an upregulated formation of adipose tissues (16). Together, these results suggest that Meltrin-α plays regulatory roles in the formation of muscle and adipose tissues.

Recently, experiments with metalloprotease inhibitors have also implicated Meltrin α in cardiac hypertrophy and in the ectodomain shedding of HB-EGF (1). Although the hearts of the Meltrin $\alpha^{-/-}$ mice appear normal, it will be of interest to test whether hypertrophy occurs under conditions of pressure overload. However, we did find that Meltrin α indeed contributes to TPA-stimulated HB-EGF ectodomain shedding in embryonic fibroblasts. The importance of HB-EGF in adipogenesis has not been examined, although its expression in interscapular mesenchymal cells has been observed (unpublished data). On the other hand, insulin-like growth factor I (IGF-I) (32) is one of the cytokines that plays an essential role in adipogenesis and stimulates myogenesis (11, 24, 25). Meltrin α interacts with IGFBP-3 and cleaves it in vitro (19, 36), suggesting that Meltrin α may also regulate the release of active IGFs in BAT and muscle cell lineages by cleaving IGFBPs.

It is not clear at this stage why the levels of penetrance of neonatal lethality, BAT malformation, and hypotrophic muscle formation are so low in the Meltrin α-null mutants. It is possible that other ADAMs may compensate for the loss of Meltrin α due to functional redundancy between Meltrin α and other ADAMs.

ACKNOWLEDGMENTS

This work was supported in part by a grant-in-aid for Scientific Research on Priority Areas from the Ministry of Education, Culture, Sports, Science, and Technology and by research grants from the Japanese Health Science Foundation, the National Center of Neurology and Psychiatry of the Ministry of Health and Welfare of Japan, and CREST (Core Research for Evolutional Science and Technology) of the Japan Science and Technology Corporation.

We thank T. Obata for technical assistance, T. Fujimori for helpful comments, and R. T. Yu for critically reading the manuscript.

REFERENCES

1. **Asakura, M., M. Kitakaze, S. Takashima, Y. Liao, F. Ishikura, T. Yoshinaka, H. Ohmoto, K. Node, K. Yoshino, H. Ishiguro, H. Asanuma, S. Sanada, Y. Matsumura, H. Takeda, S. Beppu, M. Tada, M. Hori, and S. Higashiyama.** 2002. Cardiac hypertrophy is inhibited by antagonism of ADAM12 processing of HB-EGF: metalloproteinase inhibitors as a new therapy. Nat. Med. 8:35–40.
2. **Black, R. A., C. T. Rauch, C. J. Kozlosky, J. J. Peschon, J. L. Slack, M. F. Wolfson, B. J. Castner, K. L. Stocking, P. Reddy, S. Srinivasan, N. Nelson, N. Boiani, K. A. Schooley, M. Gerhart, R. Davis, J. N. Fitzner, R. S. Johnson, R. J. Paxton, C. J. March, and D. P. Cerretti.** 1997. A metalloproteinase disintegrin that releases tumour-necrosis factor-alpha from cells. Nature 385:729–733.
3. **Black, R. A., and J. M. White.** 1998. ADAMs: focus on the protease domain. Curr. Opin. Cell Biol. 10:654–659.
4. **Blobel, C. P., T. G. Wolfsberg, C. W. Turck, D. G. Myles, P. Primakoff, and J. M. White.** 1992. A potential fusion peptide and an integrin ligand domain in a protein active in sperm-egg fusion. Nature 356:248–252.
5. **Borneman, A., R. Kuschel, and A. Fujisawa-Sehara.** 2000. Analysis for transcript expression of meltrin alpha in normal, regenerating, and denervated rat muscle. J. Muscle Res. Cell Motil. 21:475–480.
6. **Bridges, L. C., P. H. Tani, K. R. Hanson, C. M. Roberts, M. B. Judkins, and**

R. D. Bowditch. 2002. The lymphocyte metalloprotease MDC-L (ADAM 28) is a ligand for the integrin $\alpha_4\beta_1$. J. Biol. Chem. 277:3784–3792.
7. Buxbaum, J. D., K. N. Liu, Y. Luo, J. L. Slack, K. L. Stocking, J. J. Peschon, R. S. Johnson, B. J. Castner, D. P. Cerretti, and R. A. Black. 1998. Evidence that tumor necrosis factor alpha converting enzyme is involved in regulated alpha-secretase cleavage of the Alzheimer amyloid protein precursor. J. Biol. Chem. 273:27765–27767.
8. Cho, C., D. O. Bunch, J. E. Faure, E. H. Goulding, E. M. Eddy, P. Primakoff, and D. G. Myles. 1998. Fertilization defects in sperm from mice lacking Fertilin β. Science 281:1857–1859.
9. Dangain, J., and G. Vrbova. 1984. Muscle development in *mdx* mutant mice. Muscle Nerve 7:700–704.
10. Eto, K., W. Puzon-McLaughlin, D. Sheppard, A. Sehara-Fujisawa, X. P. Zhang, and Y. Takada. 2000. RGD-independent binding of integrin alpha9beta1 to the ADAM-12 and -15 disintegrin domains mediates cell-cell interaction. J. Biol. Chem. 275:34922–34930.
11. Florini, J. R., D. Z. Ewton, and S. A. Coolican. 1996. Growth hormone and the insulin-like growth factor system in myogenesis. Endocrinol. Rev. 17: 481–517.
12. Gilpin, B. J., F. Loechel, M. G. Mattei, E. Engvall, R. Albrechtsen, and U. M. Wewer. 1998. A novel, secreted form of human ADAM 12 (Meltrin α) provokes myogenesis in vivo. J. Biol. Chem. 273:157–166.
13. Goishi, K., S. Higashiyama, M. Klagsbrun, M. Ishikawa, E. Mekada, and N. Taniguchi. 1995. Phorbol ester induces the rapid processing of cell surface heparin-binding EGF-like growth factor: conversion from juxtacrine to paracrine growth factor activity. Mol. Biol. Cell 6:967–980.
14. Hogan, B., R. Beddington, F. Costantini, and E. Lacy. 1994. Manipulating the mouse embryo: a laboratory manual. Cold Spring Harbor Laboratory Press, Cold Spring Harbor, N.Y.
15. Iba, K., R. Albrechtsen, B. Gilpin, C. Frohlich, F. Loechel, A. Zolkiewska, K. Ishiguro, T. Kojima, W. Liu, J. K. Langford, R. D. Sanderson, C. Brakebusch, R. Fassler, and U. M. Wewer. 2000. The cysteine-rich domain of human ADAM 12 supports cell adhesion through syndecans and triggers signaling events that lead to beta1 integrin-dependent cell spreading. J. Cell Biol. 149:1143–1156.
16. Kawaguchi, N., X. Xu, R. tajima, P. Kronqvist, C. Sundberg, F. Loechel, R. Albrechtsen, and U. M. Wewer. 2002. ADAM 12 protease induces adipogenesis in transgenic mice. Am. J. Pathol. 160:1895–1903.
17. Kurisaki, T., A. Masuda, N. Osumi, Y. Nabeshima, and A. Fujisawa-Sehara. 1998. Spatially- and temporally-restricted expression of meltrin α (ADAM12) and β (ADAM19) in mouse embryo. Mech. Dev. 73:211–215.
18. Lieber, T., S. Kidd, and M. W. Young. 2002. Kuzbanian-mediated cleavage of *Drosophila* Notch. Genes Dev. 16:209–221.
19. Loechel, F., J. W. Fox, G. Murphy, R. Albrechtsen, and U. M. Wewer. 2000. ADAM 12-S cleaves IGFBP-3 and IGFBP-5 and is inhibited by TIMP-3. Biochem. Biophys. Res. Commun. 278:511–515.
20. Lyon, M. F., Y. Cocking, and X. Gao. 1996. Mouse chromosome atlas. Mouse Genome 95:731–798.
21. Matsuda, Y., Y. N. Harada, S. Natsuume-Sakai, K. Lee, T. Shiomi, and V. M. Chapman. 1992. Location of the mouse complement factor H gene (cfh) by FISH analysis and replication R-banding. Cytogenet. Cell Genet. 61:282–285.
22. Matsuda, Y., T. Imai, T. Shiomi, T. Saito, M. Yamauchi, T. Fukao, Y. Akao, N. Seki, H. Ito, and T. A. Hori. 1996. Comparative genome mapping of the ataxia-telangiectasia region in mouse, rat, and Syrian hamster. Genomics 34:347–352.
23. Moss, M. L., S. L. Jin, M. E. Milla, D. M. Bickett, W. Burkhart, H. L. Carter, W. J. Chen, W. C. Clay, J. R. Didsbury, D. Hassler, C. R. Hoffman, T. A. Kost, M. H. Lambert, M. A. Leesnitzer, P. McCauley, G. McGeehan, J. Mitchell, M. Moyer, G. Pahel, W. Rocque, L. K. Overton, F. Schoenen, T. Seaton, J. L. Su, J. D. Becherer, et al. 1997. Cloning of a disintegrin metalloproteinase that processes precursor tumour necrosis factor-alpha. Nature 385:733–736.
24. Musaro, A., K. McCullagh, A. Paul, L. Houghton, G. Dobrowolny, M. Molinaro, E. R. Barton, H. L. Sweeney, and N. Rosenthal. 2001. Localized Igf-1 transgene expression sustains hypertrophy and regeneration in senescent skeletal muscle. Nat. Genet. 27:195–200.
25. Musaro, A., K. J. McCullagh, F. J. Naya, E. N. Olson, and N. Rosenthal. 1999. IGF-1 induces skeletal myocyte hypertrophy through calcineurin in association with GATA-2 and NF-ATc1. Nature 400:581–585.
26. Nagy, A., J. Rossant, R. Nagy, W. Abramow-Newerly, and J. C. Roder. 1993. Derivation of completely cell culture-derived mice from early-passage embryonic stem cells. Proc. Natl. Acad. Sci. USA 90:8424–8428.
27. Nath, D., P. M. Slocombe, A. Webster, P. E. Stephens, A. J. Docherty, and G. Murphy. 2000. Meltrin γ (ADAM-9) mediates cellular adhesion through $\alpha_6\beta_1$ integrin, leading to a marked induction of fibroblast cell motility. J. Cell Sci. 113(Pt. 12):2319–2328.
28. Pan, D., and G. M. Rubin. 1997. Kuzbanian controls proteolytic processing of Notch and mediates lateral inhibition during *Drosophila* and vertebrate neurogenesis. Cell 90:271–280.
29. Pittenger, M. F., A. M. Mackay, S. C. Beck, R. K. Jaiswal, R. Douglas, J. D. Mosca, M. A. Moorman, D. W. Simonetti, S. Craig, and D. R. Marshak. 1999. Multilineage potential of adult human mesenchymal stem cells. Science 284:143–147.
30. Primakoff, P., and D. G. Myles. 2000. The ADAM gene family: surface proteins with adhesion and protease activity. Trends Genet. 16:83–87.
31. Qi, H., M. D. Rand, X. Wu, N. Sestan, W. Wang, P. Rakic, T. Xu, and S. Artavanis-Tsakonas. 1999. Processing of the Notch ligand delta by the metalloprotease Kuzbanian. Science 283:91–94.
32. Rosen, E. D., and B. M. Spiegelman. 2000. Molecular regulation of adipogenesis. Annu. Rev. Cell Dev. Biol. 16:145–171.
33. Sambrook, J., E. F. Fritsch, and T. Maniatis. 1989. Molecular cloning: a laboratory manual. Cold Spring Harbor Laboratory Press, Cold Spring Harbor, N.Y.
34. Satoh, H., M. C. Yoshida, and M. Sasaki. 1989. High resolution chromosome banding in the Norway rat, *Rattus norvegicus*. Cytogenet. Cell Genet. 50:151–154.
35. Schlondorff, J., and C. P. Blobel. 1999. Metalloprotease-disintegrins: modular proteins capable of promoting cell-cell interactions and triggering signals by protein-ectodomain shedding. J. Cell Sci. 112(Pt. 21):3603–3617.
36. Shi, Z., W. Xu, F. Loechel, U. M. Wewer, and L. J. Murphy. 2000. ADAM 12, a disintegrin metalloprotease, interacts with insulin-like growth factor-binding protein-3. J. Biol. Chem. 275:18574–18580.
37. Shirakabe, K., S. Wakatsuki, T. Kurisaki, and A. Fujisawa-Sehara. 2001. Roles of Meltrin β/ADAM19 in the processing of neuregulin. J. Biol. Chem. 276:9352–9358.
38. Somssich, I. E., and H. Hameister. 1996. Standard karyotype of early replicating bands (RBG-banding), p. 1450–1451. *In* M. F. Lyon, S. Rastan, and S. D. M. Brown (ed.), Genetic variants and strains of the laboratory mouse. Oxford University Press, Oxford, England.
39. Soriano, P., C. Montgomery, R. Geske, and A. Bradley. 1991. Targeted disruption of the c-*src* proto-oncogene leads to osteopetrosis in mice. Cell 64:693–702.
40. Sotillos, S., F. Roch, and S. Campuzano. 1997. The metalloprotease-disintegrin Kuzbanian participates in Notch activation during growth and patterning of *Drosophila* imaginal discs. Development 124:4769–4779.
41. Stedman, H. H., H. L. Sweeney, J. B. Shrager, H. C. Maguire, R. A. Panettieri, B. Petrof, M. Narusawa, J. M. Leferovich, J. T. Sladky, and A. M. Kelly. 1991. The *mdx* mouse diaphragm reproduces the degenerative changes of Duchenne muscular dystrophy. Nature 352:536–539.
42. Taylor, S. M., and P. A. Jones. 1979. Multiple new phenotypes induced in 10T1/2 and 3T3 cells treated with 5-azacytidine. Cell 17:771–779.
43. Turner, A. J., and N. M. Hooper. 1999. Role for ADAM-family proteinases as membrane protein secretases. Biochem. Soc. Trans. 27:255–259.
44. Wolfsberg, T. G., P. Primakoff, D. G. Myles, and J. M. White. 1995. ADAM, a novel family of membrane proteins containing a disintegrin and metalloprotease domain: multipotential functions in cell-cell and cell-matrix interactions. J. Cell Biol. 131:275–278.
45. Yagami-Hiromasa, T., T. Sato, T. Kurisaki, K. Kamijo, Y. Nabeshima, and A. Fujisawa-Sehara. 1995. A metalloprotease-disintegrin participating in myoblast fusion. Nature 377:652–656.
46. Yagi, T., S. Nada, N. Watanabe, H. Tamemoto, N. Kohmura, Y. Ikawa, and S. Aizawa. 1993. A novel negative selection for homologous recombinants using diphtheria toxin A fragment gene. Anal. Biochem. 214:77–86.
47. Yamada, J., T. Kuramoto, and T. Serikawa. 1994. A rat genetic linkage map and comparative maps for mouse or human homologous rat genes. Mamm. Genome 5:63–83.
48. Zhou, M., R. Graham, G. Russell, and P. I. Croucher. 2001. MDC-9 (ADAM-9/Meltrin γ) functions as an adhesion molecule by binding the $\alpha_v\beta_5$ integrin. Biochem. Biophys. Res. Commun. 280:574–580.

Activation of Adenosine A_1 Receptor Attenuates Cardiac Hypertrophy and Prevents Heart Failure in Murine Left Ventricular Pressure-Overload Model

Yulin Liao,* Seiji Takashima,* Yoshihiro Asano,* Masanori Asakura, Akiko Ogai, Yasunori Shintani, Tetsuo Minamino, Hiroshi Asanuma, Shoji Sanada, Jiyoong Kim, Hisakazu Ogita, Hitonobu Tomoike, Masatsugu Hori, Masafumi Kitakaze

Abstract—Sympathomimetic stimulation, angiotensin II, or endothelin-1 is considered to be an essential stimulus mediating ventricular hypertrophy. Adenosine is known to protect the heart from excessive catecholamine exposure, reduce production of endothelin-1, and attenuate the activation of the renin-angiotensin system. These findings suggest that adenosine may also attenuate myocardial hypertrophy. To verify this hypothesis, we examined whether activation of adenosine receptors can attenuate cardiac hypertrophy and reduce the risk of heart failure. Our in vitro study of neonatal rat cardiomyocytes showed that 2-chloroadenosine (CADO), a stable adenosine analogue, inhibits protein synthesis of cardiomyocytes induced by phenylephrine, endothelin-1, angiotensin II, or isoproterenol, which were mimicked by the stimulation of adenosine A_1 receptors. For our in vivo study, cardiac hypertrophy was induced by transverse aortic constriction (TAC) in C57BL/6 male mice. Four weeks after TAC, both heart to body weight ratio (6.80 ± 0.18 versus 8.34 ± 0.33 mg/g, $P<0.0001$) as well as lung to body weight ratio (6.23 ± 0.27 versus 10.03 ± 0.85 mg/g, $P<0.0001$) became significantly lower in CADO-treated mice than in the TAC group. Left ventricular fractional shortening and left ventricular dP/dt_{max} were improved significantly by CADO treatment. Similar results were obtained using the selective adenosine A_1 agonist N^6-cyclopentyladenosine (CPA). A nonselective adenosine antagonist, 8-(*p*-sulfophenyl)-theophylline, and a selective adenosine A_1 antagonist, 8-cyclopentyl-1,3-dipropylxanthine, eliminated the antihypertrophic effect of CADO and CPA, respectively. The plasma norepinephrine level was decreased and myocardial expression of regulator of G protein signaling 4 was upregulated in CADO-treated mice. These results indicate that the stimulation of adenosine receptors attenuates both the cardiac hypertrophy and myocardial dysfunction via adenosine A_1 receptor–mediated mechanisms. (*Circ Res.* 2003;93:759-766.)

Key Words: adenosine ■ cardiomyopathy ■ echocardiography ■ heart failure ■ myocytes

Patients with pressure-overload diseases such as systemic hypertension exhibit left ventricular hypertrophy (LVH), a major determinant of mortality and morbidity in cardiovascular diseases. It is well-known that many neurohumoral factors such as angiotensin II (Ang II),[1,2] endothelin-1 (ET-1),[3] catecholamines,[2,4] growth factors,[5,6] and tumor necrosis factor-α (TNF-α)[7] cause LVH via the activation of intracellular signal transduction mediated by calcineurin[8,9] or mitogen-activated protein kinases.[10,11]

Adenosine, a nucleoside abundantly produced by cardiac cells, is known to inhibit norepinephrine release from presynaptic vesicles,[12] reduce production of ET-1,[13] attenuate the activation of the renin-angiotensin system,[14] and counteract TNF-α.[15] Because norepinephrine, ET-1, Ang II, and TNF-α are believed to be involved in cardiac hypertrophy and remodeling,[1–4] we hypothesized that adenosine may reduce cardiac hypertrophy and improve subsequent cardiac dysfunction. Indeed, myocardial concentration of adenosine was found to markedly increase in the hypertrophied heart,[16] whereas exogenous or endogenous adenosine has been shown to inhibit the growth of rat cardiac fibroblasts in vitro.[17] We also demonstrated that the plasma concentration of adenosine increased in patients with chronic congestive heart failure (CHF)[18] and that an increase in plasma adenosine levels ameliorated CHF.[19] The enhancement of adenosine metabolism is therefore thought to improve the pathology of cardiac hypertrophy and subsequent heart failure.

Taking these findings into consideration, we postulated that sustained stimulation of adenosine receptors would be beneficial for attenuation of LVH and improvement of heart

Original received March 27, 2003; revision received August 28, 2003; accepted August 28, 2003.

From the Department of Internal Medicine and Therapeutics, Osaka University Graduate School of Medicine (Y.L., S.T., Y.A., M.A., Y.S., T.M., H.A., S.S., H.O., M.H.) and Cardiovascular Division of Internal Medicine, National Cardiovascular Center (A.O., J.K., H.T., M.K.), Osaka, Japan.

*These authors contributed equally to this study.

Correspondence to Masafumi Kitakaze, Cardiovascular Division of Internal Medicine, National Cardiovascular Center, 5-7-1 Fujishirodai, Suita, Osaka, 565-8565, Japan. E-mail kitakaze@zf6.so-net.ne.jp

Circulation Research is available at http://www.circresaha.org

DOI: 10.1161/01.RES.0000094744.88220.62

function. As far as we know, however, the role of adenosine on myocardial hypertrophy and heart function in pressure-overload state remains poorly understood. The study presented here was therefore undertaken to determine whether administration of 2-chloroadenosine (CADO), a stable analogue of adenosine, would have beneficial effects on the LV structure and heart function in a murine model of transverse aortic constriction (TAC) and, if so, to clarify the potential underlying mechanisms involved.

Materials and Methods

Agents

CADO, 8-sulfophenyltheophylline (8-SPT), phenylephrine (PE), ET-1, Ang II, isoproterenol (Iso), forskolin, N^6-cyclopentyladenosine (CPA), 8-cyclopentyl-1,3-dipropylxanthine (DPCPX), 2-*p*-(2-carboxyethyl)phenethylamino-5′-*N*-ethylcarboxamino adenosine hydrochloride (CGS21680), 5-ethylcarboxamidoadenosine (NECA), and N^6-(3-iodobenzyl)-5′-*N*-methylcarbamoyladenosine (IB-MECA) were purchased from Sigma Chemical Company.

Cell Culture for the In Vitro Study

Neonatal rat ventricular myocytes were isolated as described previously.[20] Cardiac myocytes were cultured in DMEM (Sigma) supplemented with 10% FBS (Equitech-Bio Inc). Culture media were changed to serum-free at 72 hours. Cardiomyocytes were cultured in serum-free conditions for 48 hours before experiments. Protein synthesis in cultured cells was evaluated by analysis of [^{3}H]leucine incorporation as described.[6] For cell surface area measurement, cardiomyocytes were stained with rhodamine-phalloidin and 4′,6-diamidino-2-phenylindole dihydrochloride (DAPI); confocal microscopic images (×400) were captured and surface area was measured using Scion image software (Scion Corporation).

Surgical Procedures for the In Vivo Study

Mice (C57BL/6, male, 8 to 9 weeks old, weight 18 to 25 g) were anesthetized with a mixture of pentobarbital (50 mg/kg IP) and ketamine (25 mg/kg IP). The animal model of pressure overload was created, and invasive measurement of trans-stenosis pressure gradient and left ventricular dP/dt_{max} was performed as described previously.[21–23]

Experimental Protocols I (In Vitro Study)

Cardiomyocytes were exposed to PE (10^{-4} mol/L), ET-1 (10^{-8} mol/L), Ang II (10^{-7} mol/L), Iso (10^{-5} mol/L), or forskolin (10^{-5} mol/L) for 30 hours in the presence or absence of CADO (10^{-6} mol/L), and the extent of increase in [^{3}H]leucine uptake was examined. We studied the effects of A_1 (CPA), A_{2A} (CGS21680), and A_3 (IB-MECA) receptor selective agonists and the nonselective agonist (NECA) for A_1, A_{2A}, and A_{2B} on cardiac myocyte hypertrophy.

Experimental Protocol II (In Vivo Study)

Determination of the Dosage of the Agents

Preliminary experiments were performed to determine the dosage of agents used in vivo studies. All of the agents were delivered by minipump infusion for 4 weeks (Alzet micro-osmotic pump model 1002, replaced at 2 weeks).

Roles of Stimulation of Adenosine Receptors

We treated mice with saline (TAC group), CADO alone (2 mg/kg per day), CADO (2 mg/kg per day) plus 8-SPT (10 mg/kg per day), 8-SPT alone (10 mg/kg per day), CPA (5 mg/kg per day), or CPA (5 mg/kg per day) plus DPCPX (5 mg/kg per day), respectively. Tail-cuff BP and HR measurements (BP-98A, Softron) were done at 1, 2, and 4 weeks, and the echocardiographic assessments were performed at 4 weeks after TAC. Mice were euthanized to obtain the organs for morphometric analysis. All procedures were performed in accordance with the guiding principles of Osaka University Graduate School of Medicine with regard to animal care.

Measurements of 5′-Nucleotidase Activity and the Levels of Norepinephrine and Renin

To examine whether the enzyme to produce adenosine via AMP is activated in the myocardial hypertrophic mice, we measured the myocardial 5′-nucleotidase (5′-ND) activity[24] in a time course. Plasma norepinephrine and renin levels were determined as described.[25,26]

Determination of the Expression of B Natriuretic Peptide and Regulator of G Protein Signaling 4 Using Quantitative Polymerase Chain Reaction

Total RNA was extracted from whole heart by using TRIzol reagent (GIBCO/BRL) as described by the manufacturer. Primers for quantitative polymerase chain reaction (PCR) were designed using Gene Express software (Applied Biosystems). Expression levels of natriuretic peptide precursor type B (BNP) and regulator of G protein signaling 4 (RGS-4) were determined using Quantitect SYBR Green RT-PCR kit (QIAGEN) according to the manufacturer's instruction.

Results

Chloroadenosine Inhibits Myocyte Hypertrophy Induced by the Agonists of G-Protein–Coupled Receptor

Treatment with CADO alone did not affect the basal [^{3}H]leucine uptake of myocytes when the concentration of CADO was not higher than 10^{-5} mol/L, but CADO decreased [^{3}H]leucine uptake at concentrations higher than 10^{-5} mol/L (Figure 1A). Thus, we used CADO at the concentrations of $\leq 10^{-5}$ mol/L to assess its effects on myocyte hypertrophy. Figure 1B showed that CADO inhibited PE-induced cardiomyocyte hypertrophy in a concentration-dependent fashion. Myocyte cross-sectional area was also decreased by CADO (Figures 1C and 1D). In addition, the exposure to ET-1 or Ang II induced cardiomyocyte hypertrophy, as was gauged by changes in [^{3}H]leucine incorporation, and cotreatment with CADO (10^{-6} mol/L) inhibited these G-protein–coupled receptor agonist–induced increase in [^{3}H]leucine uptake (Figure 1E).

Chloroadenosine Also Blocks Protein Kinase A–Dependent Hypertrophic Signal Pathway

Treatment of cardiomyocytes with Iso (10^{-5} mol/L) increased protein synthesis, and cotreatment with CADO dose-dependently inhibited the increase of [^{3}H]leucine uptake (Figure 2A). Cellular enlargement induced by Iso was also attenuated in CADO-treated myocytes (Figures 2B and 2C). Furthermore, treatment with forskolin, a stimulator of adenylate cyclase, also increased [^{3}H]leucine uptake, which was abolished completely by CADO at the concentration of 10^{-5} to 10^{-6} mol/L (Figure 2A).

Antihypertrophic Effect of Chloroadenosine Is Mediated by the Stimulation of Adenosine A_1 Receptors

CPA, an A_1 selective agonist, and NECA, a nonselective agonist for A_1, A_{2a}, and A_{2b} receptors, significantly inhibited the PE-induced increase of cardiac myocyte protein synthesis, but neither CGS21680, an A_{2a} receptor agonist, nor IB-MECA, an A_3 selective receptor agonist, affected the PE-

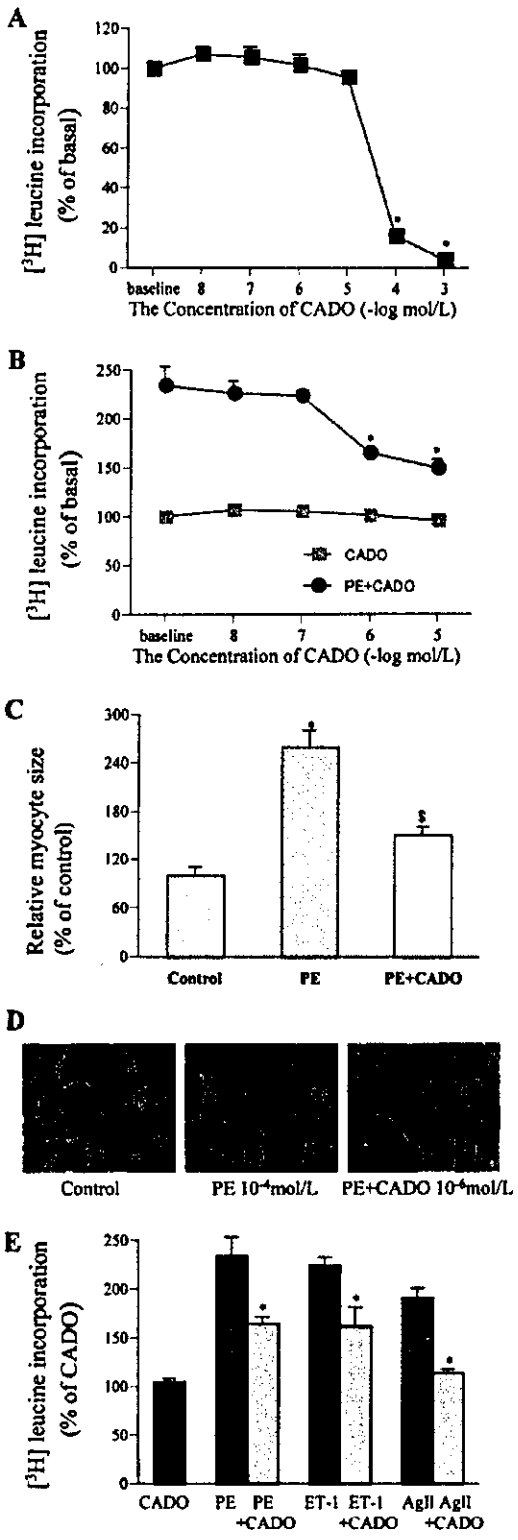

Figure 1. Inhibition of protein synthesis of myocytes by CADO. A, Concentration-dependent effects of CADO on [^{3}H]leucine incorporation in myocytes without adding stimulators. *P<0.01 compared with the value at baseline. B, Concentration-dependent effects of CADO on [^{3}H]leucine incorporation induced by PE (10^{-4} mol/L). *P<0.01 compared with the value at baseline. C, Enlargement of myocyte cross-sectional area induced by PE (10^{-4} mol/L) was decreased in the presence of CADO (10^{-6} mol/L), *P<0.01 compared with the value at control, $$P$<0.01 vs PE (n=200 cells in every group). D, Representative confocal microscopic images of myocytes with rhodamine-phalloidin staining of actin and DAPI staining of the nucleus; CADO reduced PE (10^{-4} mol/L)-induced enlargement of myocyte cross-sectional area. E, Effects of CADO (10^{-6} mol/L) on protein synthesis stimulated by PE (10^{-4} mol/L), ET-1 (10^{-8} mol/L), and Ang II (10^{-7} mol/L). *P<0.01 vs the corresponding stimulator alone. All values are expressed as mean±SEM. Every experiment was repeated at least 3 times.

induced increase of [^{3}H]leucine uptake (Figure 3A). Similar results were obtained in forskolin-induced cardiac myocyte hypertrophy (Figure 3B). Therefore, we conclude that it is A_1, not A_{2a} or A_3 receptors, that mediates the antihypertrophic effect.

Activation of Adenosine A_1 Receptors Attenuates Myocardial Hypertrophy In Vivo

Myocardial 5′-ND activity in TAC mice increased from 2 weeks after surgery and achieved significant difference at 4 weeks compared with sham-operated mice (Figure 4A). Treatment with CADO in TAC mice and plasma concentrations of norepinephrine, renin, and a molecular marker of hypertrophy BNP were significantly reduced, whereas gene expression of RGS-4, an inhibitory factor of hypertrophy, was markedly upregulated (Figures 4B and 4C). The question is whether these changes are associated with attenuated cardiac hypertrophy. Interestingly, our preliminary study showed a dose-response attenuation of cardiac hypertrophy by 1 week of treatment with CADO (Figure 5A). Along with this preliminarily study, we determined that CADO of 2 mg/kg per day is the minimal dose that exerts the maximal effects. In 4-week chronic studies, the degree of cardiac hypertrophy in CADO-treated mice was significantly lower than in TAC mice receiving vehicle treatment (P<0.0001; Figures 5B through 5F), whereas TAC led to a 74% increase in heart weight at 4 weeks after the surgery. CADO attenuated the heart weight to body weight ratio by 41% and decreased the left ventricular posterior wall thickness by 52% (Table). No significant difference was found on body weight between CADO-treated and vehicle-treated TAC mice (Table). CADO also reduced myocardial (Figure 5G) and perivascular fibrosis (Figure 5H). Meanwhile, a selective adenosine A_1 receptor agonist CPA markedly attenuated cardiac hypertrophy, and this effect was abolished by a selective A_1 receptors antagonist DPCPX (Figures 5B and 5C). Treatment with 8-SPT alone did not additionally increase cardiac hypertrophy, but cotreatment with CADO abrogated the effects of CADO on attenuating cardiac hypertrophy, as determined by the heart weight to body weight ratio and the left ventricular posterior wall thickness (Figures 5B and 5C and Table). Similarly, 8-SPT alone did not deteriorate the heart function of TAC mice, but it reversed the effects of CADO on the improvement of heart function (Figure 6A and Table).

One, two, and four weeks after the pharmaceutical treatment, systolic blood pressure and heart rate were not significantly different among all the groups, except that systolic blood pressure was slightly higher in sham group. These

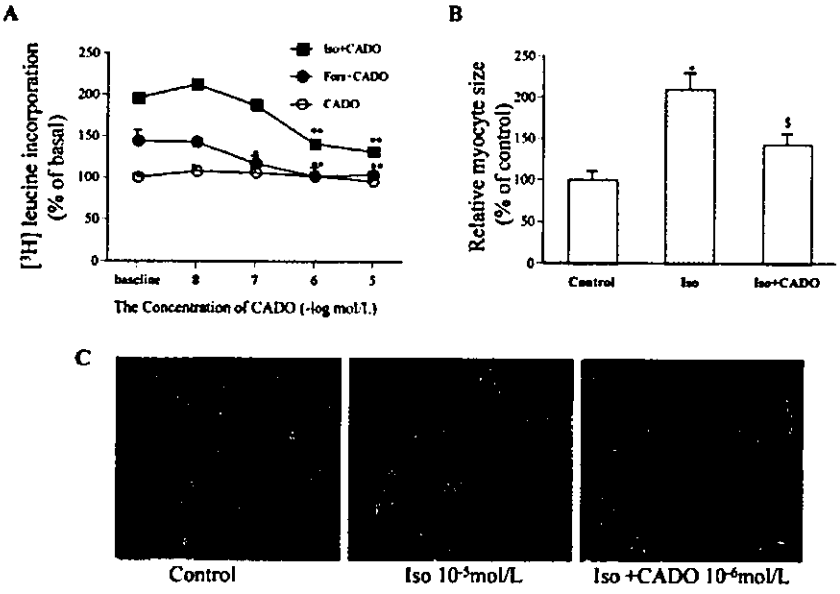

Figure 2. Inhibitory effects of CADO on protein synthesis stimulated by Iso (10^{-5} mol/L) or forskolin (Fors, 10^{-5} mol/L). A, Concentration-dependent effects of CADO on [^{3}H]leucine incorporation induced by Iso or Fors. *P<0.05, **P<0.01 compared with the value at baseline. B, Enlargement of myocyte cross-sectional area induced by Iso (10^{-5} mol/L) was decreased in the presence of CADO (10^{-6} mol/L), *P<0.01 compared with the value at control, \$$P$<0.01 vs PE (n=200 cells in every group). C, Representative confocal microscopic images of myocytes with rhodamine-phalloidin staining of actin and DAPI staining of the nucleus. Values are expressed as mean±SEM. Every experiment was repeated at least 3 times.

results may be attributed to the use of minipump to deliver the drugs in a stable and low concentration that did not significantly affect hemodynamics and also suggest that the antihypertrophic effect of CADO is independent of blood pressure change. The trans-stenosis pressure gradients were similar in all the mice that received TAC treatment. The results of hemodynamics at 4 weeks are shown in the Table.

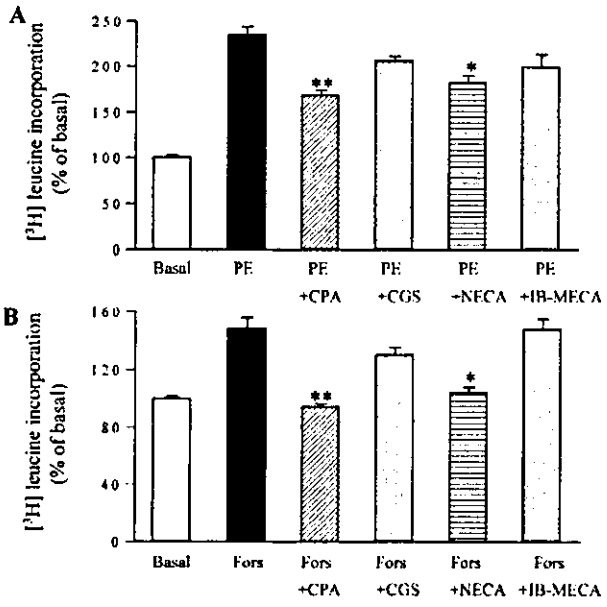

Figure 3. Effects of adenosine receptor agonists on myocyte hypertrophy induced by PE (A) or forskolin (B). Values are expressed as mean±SEM, *P<0.05, **P<0.01 compared with PE or forskolin alone. Every experiment was repeated at least 3 times. Concentration of PE and forskolin was 10^{-4} and 10^{-5} mol/L, respectively; concentration of other agents is 10^{-6} mol/L; CGS indicates 2-*p*-(2-carboxyethyl) phenethylamino-5′-*N*-ethylcarboxamino adenosine hydrochloride.

Activation of Adenosine A_1 Receptors Prevents Heart Failure In Vivo

Pressure overload induced CHF manifested by increases in the lung weight and reduction in fractional shortening (FS) and LV dP/dt_{max}. In TAC mice, the lung weight to body weight ratio increased by an average of 93%, the treatment with CADO markedly ameliorated pulmonary congestion by ≈80%, and even no significant difference was found on the lung weight to body weight ratio between CADO-treated TAC mice and sham-operated mice (Figures 6A and 6B). Comparable results are also observed in CPA-treated TAC mice (Figure 6A). We defined lung weight to body weight ratio higher than mean±4 SD in sham mice as the criteria for pulmonary congestion; consequently, the incidence of pulmonary congestion was 62% (16 of 29) in saline-treated TAC mice, which is dramatically higher relative to 15% (3 of 20) in CADO-treated TAC mice (P=0.0013). FS and LV dP/dt_{max} also increased in either CADO- or CPA-treated mice compared with saline-treated TAC mice (Figures 6C and 6D). Linear correlation analysis noted a significant positive correlation between the heart weight to body weight ratio and the lung weight to body weight ratio (r=0.857, P<0.001).

Discussion

In this study we were able to demonstrate for the first time that the stimulation of adenosine receptors can effectively attenuate myocyte hypertrophy in vitro and in vivo and improve functioning of the pressure-overloaded heart. Our findings also suggest that these beneficial effects on cardiac hypertrophy and heart function are mediated by adenosine A_1 receptors.

As shown in this study, the stimulation of adenosine receptors attenuated G-protein–coupled receptor–induced cardiac hypertrophy in vitro, which suggests that adenosine receptor–induced intracellular signaling may interfere with the cardiac hypertrophic signaling. To clarify this issue, we examined what type of adenosine receptors is involved in this

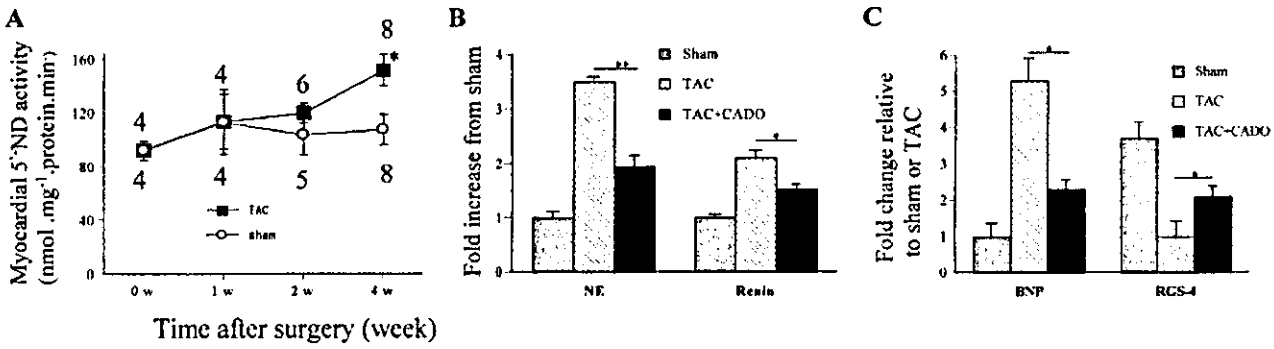

Figure 4. Results of 5′-ND, norepinephrine, renin, and expression of RGS-4 and BNP. A, Time course of myocardial 5′-ND activity. *$P<0.05$ compared with the sham-operated mice. The number of mice in each time point is indicated above or under the data points. B, Plasma concentrations of NE and renin (n=7 in each group), *$P<0.05$, **$P<0.01$ compared with TAC. C, Fold change of gene expression of BNP and RGS-4 (n=4 in each group), *$P<0.05$ compared with the sham-operated mice. Values are expressed as mean±SEM.

phenomenon. Considering that the EC_{50} of CADO on adenylate cyclase activity mediated by A_1, A_{2A}, and A_{2B} receptors is 100, 460, and 15 000 nmol/L, respectively, and the inhibitory effects of CADO are mimicked by CPA (A_1 receptor selective agonist) and NECA (A_1, A_{2A}, and A_{2B} receptor agonist) but not CGS21680 (A_{2A} receptor selective agonist), the inhibitory effects of adenosine on protein synthesis are most likely mediated via A_1 receptors rather than A_{2A} receptors. However, mediation via the A_{2B} receptor cannot be completely ruled out because the low affinity of CADO for the A_{2B} receptor makes it unlikely that the stimulation of A_{2B} receptors mediates myocardial antihypertrophy produced by CADO. Furthermore, our in vivo studies using a selective adenosine A_1 agonist, CPA, and an antagonist, DPCPX, clearly showed that the stimulation of A_1 receptors mainly mediates the antihypertrophic effect of CADO. Moreover, there is a substantial

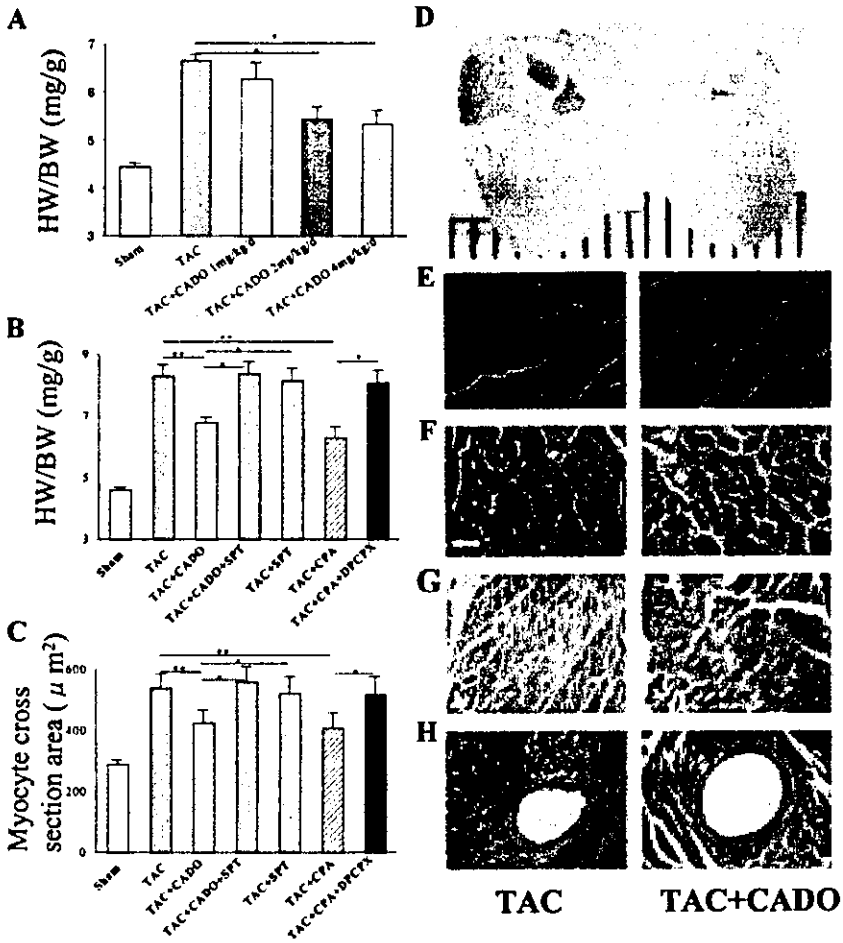

Figure 5. Inhibition of myocardial hypertrophy and fibrosis in vivo by CADO. A, Heart weight to body weight (HW/BW) ratio was attenuated in a dose-dependent fashion by CADO after 1 week of TAC. *$P<0.05$, n=10 and 7 in sham and TAC groups, respectively; n=5 in the 3 different dose CADO groups. B, HW/BW was attenuated by CADO or CPA treatment after 4 weeks, *$P<0.01$, **$P<0.0001$. The number of mice in sham, TAC, TAC+CADO, TAC+CADO+SPT, TAC+SPT, TAC+CPA, and TAC+CPA+DPCPX groups is 28, 29, 20, 8, 12, 5, and 6, respectively. C, Cardiomyocyte cross-sectional area was decreased in CADO- or CPA-treated mice after 4 weeks, *$P<0.05$, **$P<0.01$. The number of mice in sham, TAC, TAC+CADO, TAC+CADO+SPT, TAC+SPT, TAC+CPA, and TAC+CPA+DPCPX group is 9, 11, 8, 5, 6, 5, and 6, respectively. D, Representative hearts of mice treated with TAC or TAC+CADO for 4 weeks (scale bar=1 mm). E and F, H&E staining of heart tissues (scale bar=20 μm). Myocardial (G) or perivascular (H) fibrosis (Azan-Mallory stain, bar=20 μm). Values are mean±SEM.

Hemodynamics and Echocardiographic Results at 4 Weeks

	TAC (n=22)	TAC+SPT+CADO (n=7)	TAC+SPT (n=17)	TAC+CADO (n=15)	TAC+CPA (n=6)	TAC+CPA +DPCPX (n=6)	Sham (n=14)
BW, g	23.2±0.47†	21.1±0.31†	22.5±0.46†	22.6±0.34†	22.8±0.44†	22.2±0.6†	24.6±0.24
HR, bpm	645±26.8	614±32.6	678±22.2	643±11.4	680±17	680±18	671±11.4
SBP, mm Hg	104±3.7	104±3.7	102±3.1*	107±1.8	100±8	94±5*	114±3.0
δBP, mm Hg	51±6	49±4	49±5	47±6	48±5	46±7	5±3
PWTd, mm	1.04±0.05†§¶	0.99±0.02†§	1.01±0.06†§	0.85±0.03†	0.75±0.01	0.94±0.04†#	0.66±0.02
LVEDd, mm	3.35±0.13*‡¶	3.34±0.15*‡	3.35±0.16*‡	3.24±0.10	3.21±0.09	3.47±0.13*¶	3.16±0.12
LVESd, mm	2.30±0.14*‡¶	2.32±0.15*‡	2.31±0.18*‡	2.06±0.10	1.98±0.11	2.35±0.15*¶	1.95±0.12
%PWT	24.8±4.2†§¶	23.4±3.3†§	28.8±6.5	41.4±4.5	42.3±5.2	22.7±6.4†¶	42.7±7.6

SPT indicates 8-(*p*-sulfophenyl)-theophylline; HR, heart rate; SBP, systolic blood pressure; δBP, *trans*-stenosis pressure gradient (n=3 to 4 in every group); TAC, transverse aortic constriction; PWTd, left ventricular (LV) diastolic posterior wall thickness; LVEDd, LV end-diastolic dimension; LVESd, LV end-systolic dimension; %PWT, percentage of increase in PWTs relative to PWTd; and FS, left ventricular fractional shortening. *$P<0.05$, †$P<0.01$ vs Sham; ‡$P<0.05$, §$P<0.01$ vs TAC+CADO; ¶$P<0.01$ vs TAC+CPA. Data are mean±SEM.

body of evidence suggesting that the stimulation of A_1 receptors mediates antigrowth effect. Adenosine-induced inhibition of norepinephrine release from adrenergic nerves in the heart is also mediated via the A_1 receptor[27] and has an antiadrenergic effect on hypertrophy caused by pressure overload,[16] consistent with the result in this study that plasma norepinephrine was reduced by CADO treatment. Interestingly, the activation of adenosine A_1 receptors has been reported to be able to inhibit cardiac cell proliferation and lead to cardiac hypoplasia in cultured whole murine embryos.[28] We were also able to demonstrate in this study that CADO can inhibit protein kinase A–dependent hypertrophic signaling. Iso stimulates hypertrophy by activation of adrenergic β receptors, and this stimulation leads to the activation of adenylate cyclase and subsequently induces hypertrophy. The stimulation of adenosine A_1 receptors is known to inhibit adenylate cyclase, which therefore may be an alternative mechanism for CADO-induced attenuation of hypertrophy. To clarify this point, we used forskolin, the most potent AC stimulator, to stimulate protein synthesis of myocytes. As expected, CADO completely eliminated any increase in the protein synthesis induced by forskolin. We therefore posit that the signaling of A_1 receptor activation is linked with both G_o and G_i proteins and that inhibition of adenylate cyclase may suppress the hypertrophic signaling pathways in cardiomyocytes.

It has become clear that the development of cardiac hypertrophy is a multigenic, integrative response involving signal integration of multiple pathways. The antihypertrophic effect of CADO could also be attributable, in part, to a reduction of $[Ca^{2+}]_i$ in myocytes,[16] because $[Ca^{2+}]_i$ can stimulate the calcineurin-mediated cardiac hypertrophic pathway.[9] Even more interesting is that RGS, which attenuates G protein–mediated signaling, may also be an alternative pathway through which CADO can inhibit G_q protein–induced hypertrophy, because it is reported that an increase in cAMP level resulted in a reduction of the RGS-4 message by nearly 50%.[29] We also confirmed in this study that expression of RGS-4 was upregulated by CADO treatment. Thus, CADO may exert an antihypertrophic effect mediated by increasing RGS-4 via the inhibition of adenylate cyclase.

Our results indicate that CADO not only attenuates cardiac hypertrophy but also dramatically improves heart function, which is consistent with our findings in patients with heart failure as previously reported.[19] The antiadrenergic effect of CADO is likely to protect the heart in a way similar to that of the adrenergic β blocker by reducing either contractility or heart rate. Moreover, CADO may be superior to β blocker because it can attenuate the activation of renin-angiotensin system[14] and counteract TNF-α.[15] On the other hand, we also should notice that A_1 adenosine antagonist BG9719 was reported to preserve renal function via promoting natriuresis during treatment for heart failure.[30] Reducing glomerular filtration rate should be considered one of the adverse effects of adenosine A_1 agonists, but it is not enough to deny the potential beneficial affects of adenosine receptor activation on heart failure mediated by their well-known antiadrenergic effect. Nevertheless, a recent study revealed that no significant difference on glomerular filtration rate was noted between A_1 receptor deficiency mice and wild-type mice.[25] In this study, we have noted a positive correlation between cardiac hypertrophy and pulmonary congestion, indicating that the beneficial effect of CADO on preventing heart failure at least partially should be attributed to its inhibitory effect on myocardial hypertrophy. Although this seems paradoxical to the traditional notion that hypertrophy is a needed compensatory mechanism, recent studies on murine TAC model suggest that cardiac hypertrophy is not a required compensatory response to pressure overload.[31,32]

We have characterized the time course of LVH and heart function changes in a previous study[21] and showed that significant LVH and impaired LV heart function (FS) appeared at 4 weeks after TAC. In this study, we noted that myocardial 5′-ND activity was also increased significantly at 4 weeks, a time course in good accordance with FS, suggesting that declined heart function is associated with increased 5′-ND activity. This observation is in agreement with the clinical investigation.[18] Although in this study we did not find that 8-SPT additionally increases cardiac hypertrophy and decelerates the heart function in the TAC model, the cardioprotection of adenosine cannot be excluded because the concentration of endogenous adenosine may be far below the